TECHNICAL REPORT

ASSESSING POTENTIAL RELATIONSHIPS BETWEEN TOPOGRAPHIC ATTRIBUTES AND SOIL TEXTURE CHARACTERISTICS FOR GRANITIC SOILS OF NORTH-CENTRAL COLORADO

Submitted by

Kevin A. Wickham

Department of Civil and Environmental Engineering

In partial fulfillment of the requirements

For the Degree of Master of Science

Colorado State University

Fort Collins, Colorado

2023

Master's Committee:

Advisor: Jeffrey D. Niemann

Co-Advisor: Joseph Scalia IV

Lisa Stright

Abstract

Soil characteristics are critical variables in various settings from vehicle mobility and terrain trafficability to crop viability. Predicting these characteristics has become more important as climate and weather patterns change. Two defining aspects of soil characterization are soil moisture and soil strength. Methods have been proposed to estimate both and are being tested at Maxwell Ranch, however, these methods depend upon soil texture, which is difficult to observe and estimate across highly variable regions. The study area was Maxwell Ranch in North-Central Colorado, a highly topographically variable region. Lab analysis determined soil textures and their respective classifications from collected soil samples. The resulting data was analyzed via linear regressions and multiple linear regressions. The objective of this report is to assess the predictability of soil texture based on relationships to vegetation and topography in a highly variable region. Several relationships between soil textures, topography, and vegetation were observed. The natural log of contributing area was positively correlated and slope was negatively correlated with percent fines across most regions. Eastness was positively correlated and summer sun exposure was negatively correlated with particle diameter percentiles and percent gravel. Vegetation type played a significant role in correlation, with grass and shrub-type vegetation correlating while tree-type vegetation did not. Multiple linear regression weighed slope, curvature, Eastness, winter sun exposure, and vegetation the most heavily across most regions.

Introduction

Assessing vehicle mobility is a challenge in any application requiring a vehicle to traverse natural terrain. Evaluating and predicting that trafficability is crucial to agriculture, forestry, and military applications. Military applications have driven the need for further evaluation, as concerns about terrain trafficability led to the first formal mobility analyses after soft, wet soils caused vehicle immobilization in World War II (Rula and Nuttall, 1971). The U.S. Army and the North Atlantic Treaty Organization (NATO) developed several iterations of a military mobility model dubbed the NATO Reference Mobility Model (NRMM) to assist in military operations planning. The most recent iteration is termed the Next-Generation NATO Reference Mobility Model (NG-NRMM) and updated equations and methods to incorporate computer technology and model advancements (Bradbury et al., 2016). Within all these models, three major concepts are involved in the study of terrain trafficability: the vehicle, the driver, and the terrain (Rula and Nuttall, 1971). Within terrain, slope, soil texture, general vegetative cover, soil moisture content, soil strength, surface roughness, soil types and distributions, and other obstacles (e.g., vegetation, water) are analyzed to determine optimal routing and attainable speeds. Soil strength is a critical variable in the evaluation and prediction of off-road vehicle mobility. Soil strength is controlled by several soil characteristics, including texture (percentage of sand, silt, and clay), density, water content, and organic matter content. Therefore, accurately characterizing soil textures is essential to vehicle mobility analysis.

Determining soil textures comes with considerable difficulty. They are the result of a complex web of environmental and management factors that can form seemingly random outcomes. Within environmental factors alone come several reasons for the difficulty of determination: complexity, variability, scale, measurement methods, and soil horizons (Channarayappa, 2019). Soil is a complex, three-dimensional matrix of mineral particles, organic matter, air, and water, and can be influenced by factors such as climate, geology, topography, vegetation, and human activities. Variability is highly dependent on location and scale, as soil textures vary significantly across short extents, with 30% of spatial variability occurring under 1 km, and 50% occurring under 10 km (Paterson et al., 2018). Soil textures are typically determined through laboratory analysis, with different methods potentially yielding different results, making comparing data from different studies challenging. Soil horizons are the different layers within soils, which can have drastically different properties (e.g., the texture of topsoil may differ from the texture of subsoil due to variations in organic matter and mineral content)

(Channarayappa, 2019). These variables make soil texture determination difficult and warrant an investigation into the potential correlation between soil textures and their inputs.

Remote sensing is defined as the acquisition and measurement of information with a device not in contact with features under surveillance (Khorram, 2012). This surveying and data collection technique typically refers to aircraft or satellite technologies that record electromagnetic energy. All objects have a particular emission and/or reflectance property, known as a spectral signature, and thus can be distinguished from other objects. The advantages of these systems are the ability to capture large areas with a single observation, a regular cycle of observation to observe changes, and precise geographic location mapping. Remote sensing data is generally input into Geographic Information Systems (GIS), which can be used to store, manipulate, and analyze the data (Khorram, 2012). For example, red and near-infrared light are wavelengths that can be measured and processed to estimate vegetation in a grid cell. Several advancements in these technologies and methodologies have made the prediction of soil textures more accurate if not infallible. Accurate is defined by comparison to in-situ field reference data (Khorram, 2012). Spectroscopy, the measurement and analysis of spectral signatures, has been shown to have accuracy and quality similar to traditional soil analytical methods when predicting soil physical and chemical properties (Kopačková et al., 2017, Pinheiro et al. 2017). However, while some properties were estimated with high accuracy, others were poorly predicted. A methodological advancement in the combination of hyperscale digital elevation mapping (DEM) and local morphometric variables (LMV) has led to even more accurate predictions of soil texture, but there are severe limitations around terrain variability (Riza et al., 2021). DEMs are models of various topographic attributes (e.g., slope), and hyperspectral DEMs use a wider spectrum of light compared to the standard DEMs assigning primary colors to each pixel. Local morphometric variables are mathematical parameters that describe the shape and characteristics of a particular location on the earth's surface (Florinsky, 2016). These are commonly derived from DEMs and can be used to quantify local terrain features (e.g., slope, aspect, curvature, elevation). The combination of these as described by Riza et al. (2021) lead to improved soil texture prediction accuracy, but high levels of terrain variability cause a substantial decrease in that accuracy. The objective of this report is to determine the predictability of soil texture based on potential relationships to vegetation and topography in a highly variable region.

Methodology

The research area for this report was Maxwell Ranch in North-Central Colorado as shown in Fig. (1.1). It is a 4000-hectare cattle ranch 53 km northwest of Fort Collins, Colorado. It is in the Laramie foothills at the transition between the mountains and plains, and has thin soils derived from weathered granite and sandstone and herbaceous vegetation with scattered shrubs (Mountain Mahogany) and trees (Ponderosa Pine). This ranch was chosen for its high variability in topography, vegetation, and geographic location. Eighty-six selected soil collection sites captured all unique soil topography and vegetation across the ranch. Site locations included both wet and dry peaks and valleys. Several streams run through the ranch, with several collection sites located near running water. The ranch was split into four segments (Fig. 1.2): Regions A (Fig. 1.3), B (Fig. 1.4), C (Fig 1.5), and D (Fig 1.6), with A and D bordering the north and south edges of the ranch respectively with B and C being central northeast and central southwest respectively (Fig. 1.2). Weather in the region differed from region to region. Wind generally blew out of the southwest, with some gusts coming from directly south or east. Storms also came out of the southwest, but cloud cover often split at the western border of regions C and D, circumventing the ranch entirely and leading to anecdotally drier land than the surrounding ranches. Region A's vegetation consisted of shrubs and grasses, with several areas of deep, marshy grasses. Region B's vegetation was unique amongst the regions, consisting mostly of tree cover with some thinly spread shrubs and two grassy, stream-adjacent sites. Region C's vegetation was spread thinly across much of the region, with half the sites having sparse grasses, nearly half the sites having tree cover, and two points in deep, marshy grasses. Region D's vegetation was mainly shrubs with two sites in deep grasses. Regions A and C were the only ones with multiple collection sites in marshy grasses. Regression analysis was conducted collectively over the entire ranch and subsequent analysis was performed over individual regions. Ranch-wide assessments give context and characterization for the whole area and can give insight into the accuracy of regional representation. Regional assessments capture and weigh variability on a smaller scale and can reveal relationships that may be dampened or nonexistent in the study of the entire area. Collectively, these assessments capture trends in variable predictability and characterizes these trends in terms of how broadly soil textures can be predicted.

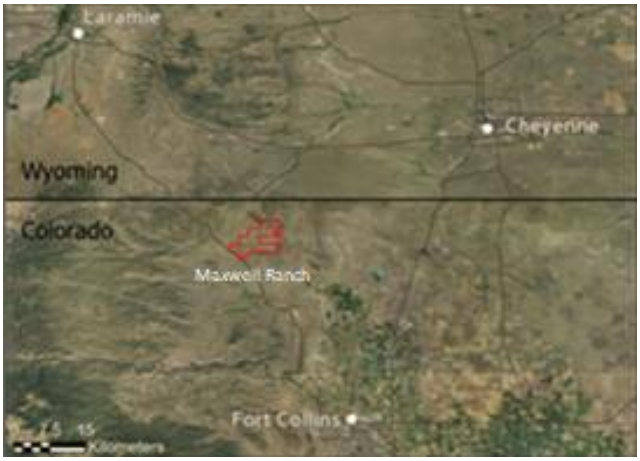

Fig. 1.1. *Maxwell Ranch located in North-Central Colorado (Obtained from Sami Fischer and Matt Bullock)*

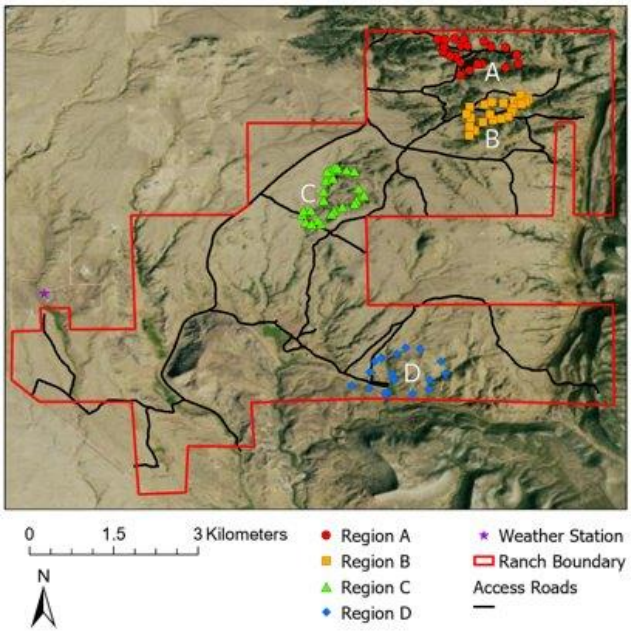

Fig. 1.2. *Maxwell Ranch delineated into Regions A, B, C, and D (Obtained from Sami Fischer and Matt Bullock)*

Fig. 1.3. *Region A on the Northern Edge of the Ranch*

Fig. 1.4. *Region B on the Central Northeast Area of the Ranch*

Fig. 1.5. *Region C on the Central Northwest Area of the Ranch*

Fig. 1.6. *Region D on the Southern Edge of the Ranch*

Topographic characteristics and vegetation are independent variables and have a considerable impact on mobility. Within the broad scope of terrain characteristics provided by Rula and Nuttall (1971), this report will study the independent variables slope, contributing area, elevation, orientation, curvature, and general vegetative cover. Slope, contributing area, and elevation are pulled directly from the Terrain Analysis Using Digital Elevation Models (TauDEM). The values for these variables are given in the form of grid cells. Slope is evaluated in the direction of steepest descent and reported as the elevation change over the grid cell (Tarboton, 2004). Contributing area refers to the summation of a grid cell's contribution and the contributions upslope that drain into it, resulting in the area draining to testing locations. The natural log of contributing area was used to normalize the data. Aspect is a GIS output raster derived from an input elevation raster and refers to the compass direction a slope is facing (Hofmann-Wellenhof et al., 2001, Eberly, 1991, Krakiwsky et al., 1971, Lancaster, 1986, Ligas, 2011). Orientation, while generally being interchangeable with aspect, will be defined in this report as a calculation involving both slope and aspect that results in a value describing how much exposure a slope has to a given direction, referred to as the "Northness" and "Eastness" of a given slope. For instance, if a given slope has a larger Northness value, it will be more exposed to the north. Northness is calculated: N = Slope * Cos (Aspect) and is related to the amount of shading or sun a point receives. Eastness is calculated: E = Slope * Sin (Aspect) and is related to wind exposure as the wind on the ranch generally comes from the west. Insolation refers to the quantity of solar radiation received on a surface, and its intensity is heavily influenced by aspect and slope (Lee, 1964). Potential Solar Radiation Index (PSRI) is the ratio of insolation on a sloping surface to the insolation on a horizontal surface at the same location and time. While its intended purpose is to be an estimator of evapotranspiration, it is a function of watershed orientation and thus an important measure of topography. Two dates were selected to maximize and minimize the angle of incident solar radiation in the 06/21/2022 Summer Solstice and 12/21/2022 Winter Solstice (WS) respectively. Vegetation indices, the last two sets of independent variables considered in this report, are Normalized Difference Vegetation Index (NDVI) and Soil Adjusted Vegetation Index (SAVI). NDVI quantifies vegetation greenness through a ratio between the red (R) and near-infrared (NIR) reflectances via the calculation: (NIR - R) / (NIR + R) (Masek et al., 2006; Vermote et al., 2016). SAVI is a corrected vegetation index that accounts for the influence of soil brightness where vegetative cover is low using a soil brightness correction factor. Three sources of these vegetation indices were included in this report with no overlap in dates: Sentinel-2 (S2), Landsat (LS), and Planet Cube Sat (PCS). Different dates were used to represent changes in vegetation over time and the selected dates were those with a clear image with low cloud cover. LS has a 30 m resolution, S2 has a 10 m

resolution, and PCS has a 3 m resolution. All are delivered from USGS as GIS single-band products. Single-band products are the simplest version of a raster file with there being only a single layer of raster values.

Fig. 1.7. *Left to Right: Handheld GPS recording at each soil collection location, Soil collection with a trowel, Bulk density volume measurements with a Rubber Balloon*

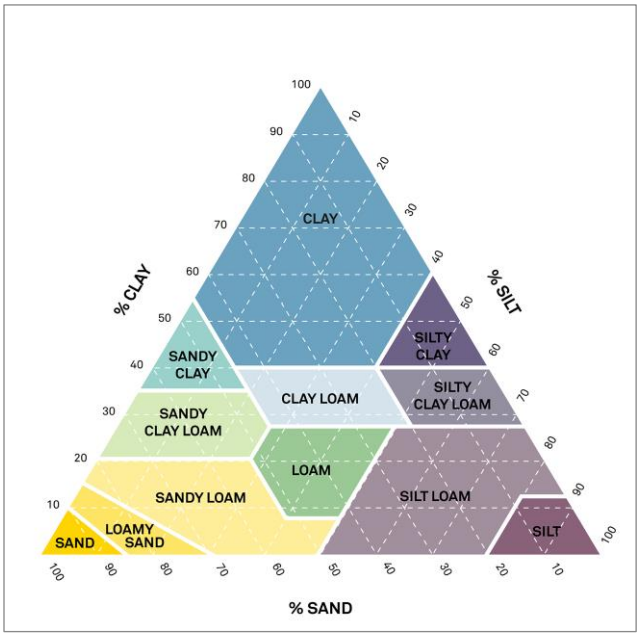

Fig. 1.8. *USDA Soil Classification Triangle (METER, 2021)*

Field and Laboratory Analysis Methods

Soil texture characterization is composed of several American Society for Testing and Materials (ASTM) standards, which are published voluntary consensus technical standards that define various procedures to obtain specific data used in texture characterization. ASTM D6913-09 dictates minimum soil mass collection based on the largest particle size and separates the mass of particles of a sample between 75 mm and 75-µm into size ranges. ASTM D7928-21E01 determines the mass of particles of a sample under 75-µm via a sedimentation process using a hydrometer. ASTM D2216-10 determines the water content of a sample through a reduction in mass by oven-drying (110°C) and subsequent calculation. Once these procedures are complete, the series of data output from the hydrometer is used via Fig. (1.8) to determine USDA soil texture classification. ASTM D2487-17e1 utilizes data on particles under 75-µm to determine USCS soil classification. These ASTMs result in a series of soil texture data that are evaluated for relationships with the topography of their respective soil collection locations.

The "Standard Test Methods for Particle-Size Distribution (Gradation) of Soils Using Sieve Analysis" (ASTM D6913-09) dictates minimum soil mass collection based on the largest particle size and separates the mass of particles of a sample between 75-mm and 75-µm into size ranges. The minimum allowable moist soil mass is based on visual maximum particle size as defined in Table (1.1). Due to field limitations of individual persons' carrying capacity and soil collection bag sizes (1 kg), the minimum mass had to be modified. The ASTM calls for 3 kg for samples whose largest particle was retained on the 25.4 mm sieve and 10 kg for those whose largest particle was retained on the 38.1 mm sieve. Standard soil collection moist masses for this report varied between 600-800 grams due to visual estimation of sufficient mass per bag. 100-150 grams of the total sample for each location were prepared for the mechanical sieve via taring (weighing the sample container) and weighing the moist sample. These samples were oven-dried to a standard 110 $\pm$ 5°C and weighed with the loss of mass considered water loss. The samples are then washed over a No. 200 sieve (75 µm), which removes any particles smaller than 75 µm in diameter. These smaller particles can cause significant errors in the mechanical sieve results by adding masses to any given sieve layer. Once washed, the samples are oven-dried and weighed again before being manually sieved through the 38.1 mm and 25.4 mm sieves. The 76.2 mm sieve was not used because no sample contained particles large enough, and thus this sieve could be skipped. The processing through the two sieves was completed manually due to the ease of passing these sieves and the mechanical sieve not being required. The remaining sample was placed into a sieve stack and masses collected on individual sieves were recorded (Table 1.2) and used for USCS

classification (ASTM D2487-17e1). Classification procedure dictates a fine-grained soil if 50% or more dry mass passes the No. 200 sieve, a coarse-grained soil if 50% or more dry mass is retained on the No. 200 sieve, and further sub-classifications are defined within those (Table 1.2).

Table 1.1. *Minimum Requirements for Mass of Test Specimen, and Balance Readability (ASTM D6913-09). Note: Balance Readability is the precision of a balance.*

Maximum Particle Size (100 % Passing)		Method A: Water Content Recorded to $\pm$ 1 %		Method B: Water Content Recorded to $\pm$ 0.1 %	
SI Unite Sieve Size	Alternate Sieve Size	Specimen Mass	Balance Readability (g)	Specimen Mass (g)	Balance Readability (g)
75.0 mm	3 in.	5 kg	10	50 kg	10
37.5 mm	1-1/2 in.	1 kg	10	10 kg	10
19.0 mm	3/4 in.	250 g	1	2.5 kg	1
7.5 mm	3/8 in.	50 g	0.1	500 g	0.1
4.75 mm	No. 4	20 g	0.1	100 g	0.1
2.00 mm	No. 10	20 g	0.1	20 g	0.01

Table 1.2. *Sieve Stack Sizes used for USCS particle distribution.*

Sieve No.	**USCS Classification**
1-1/2" (38.1 mm)	Gravel
1" (25.4 mm)	
3/4" (19.0 mm)	
3/8" (9.5 mm)	
#4 (4.76 mm)	
#10 (2 mm)	Coarse Sand
#20 (841 µm)	Medium Sand
#40 (400 µm)	
#60 (250 µm)	Fine Sand
#100 (150 µm)	
#200 (75 µm)	
Pan	
Sample removed in washing	**Fines**

The "Standard Test Method for Particle-Size Distribution (Gradation) of Fine-Grained Soils Using the Sedimentation (Hydrometer) Analysis" determines the particle-size distribution of materials finer than the No. 200 (75-µm) sieve (ASTM D7928-21E01). This ASTM's results must be combined with a sieve analysis (ASTM D6913-09) to obtain a complete particle size distribution for a sample. This method is performed on material passing the No. 10 (2 mm) sieve and requires at least 15 g of material in the sedimentation specimen. A targeted mass of 45-50 g of moist mass per sample was determined sufficient for this test. Each sample was mixed with 5 $\pm$ 0.1 grams of sodium hexametaphosphate (dispersing agent) with approximately 100 mL of deionized water and transferred into the mixing cup (Fig. 1.9). Hydrometers measure the density and specific gravity of a liquid at a certain depth. A dispersing agent is required to break up the fine-grained particles of a sample so that the liquid mixture can be more representative of the sample mass's true characteristics. Additional deionized water was added to fill the mixing cup approximately half full and mixed for 1 minute. This dispersed sample was then transferred to a metered sedimentation cylinder (graduated glass cylinder capable of holding up to 1000 mL accurately) and filled to the 1000 mL mark with deionized water. The samples were turned tip

over tail and back for 1 minute and left overnight for temperature equilibrium and deflocculation. Deflocculation is the dispersal of soil into very fine particles. After 24 hours, the samples would be turned tip over tail for 1 minute and a hydrometer would be placed into the sedimentation cylinder. The hydrometers used were the PARIO Automated Hydrometers (METER, 2021) from METER Group AG (Fig. 1.10).

Hydrometer measurements are based on Stokes' Law, which defines particle sedimentation velocity as a function of particle size and density (Durner, 2017). The hydrometer method relies on measuring temporal changes in particle concentration or density of a suspended liquid at a selected depth, or measurement location. PARIO uses a method based on the pressure in the suspension at a measurement location, which is a measure of the particles in suspension above the measuring depth. The observed data is compared to a simulated series of data and yields a high-resolution particle size distribution (Durner, 2017). This data must go through a final post-processing step to determine sand content via a final fit to measured sieve fractions for the cumulative particle size distribution to be correct. To obtain the sieve fractions, the sample from the hydrometer is washed through the No. 35 (500 µm), No. 60 (250 µm), and No. 270 (53 µm) sieves. These three samples are transferred into three tared containers, oven-dried at 110 $\pm$ 5°C, and weighed again to obtain the mass percentage of each size distribution (Table 2.3). These percentages are input back into the PARIO program as sieve fractions and the data, once fitted, gives the USDA classifications .

Table 2.3. *USDA Sand Particle Size Classifications Used for PARIO Post-Processing*

Particle Size	**USDA Classification**
53 – 250 µm	Fine Sand
250 – 500 µm	Medium Sand
500 – 2000 µm	Coarse Sand

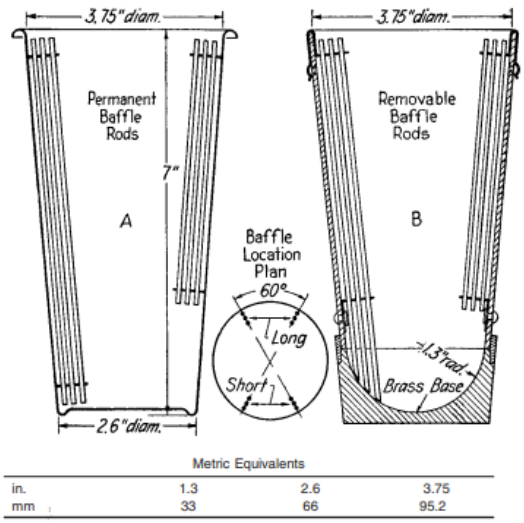

Fig. 1.9. *Dispersion Cups of Apparatus (ASTM D7928-21E01)*

Fig. 1.10. *PARIO Automated Hydrometer from METER Group AG (METER, 2021)*

These procedures produce a range of soil particle sizes and soil classifications for USCS and USDA. To characterize the relationship between the particle sizes and topography, several representative diameter percentiles were chosen. These percentiles are written in the form “D10” for the 10th percentile particle diameter of a given sample, and an effective range of particle sizes is achieved by subtracting the 10th percentile from the 90th percentile in the form “D90-10”. Two final soil

variables are determined via the Cosby et al. (1984) calculation that uses USDA classification percentages to estimate porosity and hydraulic conductivity. Porosity is calculated: $50.5 - 0.142 * (\%\ \text{Sand}) - 0.037 * (\%\ \text{Clay})$. Hydraulic Conductivity in mm/day is calculated: $(e^{-0.6+0.0126*(\%\ Sand)-0.0064*(\%\ Clay)} * 2.54 * 10 * 24)/0.00164042$. While these are both derived from % Sand and % Clay, there are several ways hydraulic conductivity and porosity's trends could diverge. While generally if pores are large and well-connected, water can flow through the soil easily and hydraulic conductivity will be high, this is not always the case. If the pores are small or not well-connected, water may not be able to flow as easily, and hydraulic conductivity will be lower. Clay particles can also restrict water flow, resulting in high porosity and low hydraulic conductivity. These particle size distributions, soil classifications, and pedotransfer function outputs sum to 14 dependent variables: D10, D30, D50, D60, D90, D90-10, percent gravel (USCS), percent sand (USCS), percent fines (USCS), percent sand (USDA), percent silt (USDA), percent clay (USDA), porosity, and hydraulic conductivity. General sizing terms for classifications are defined in Table (2.4) and used throughout the report. Any percent sand will have its respective classification stated (e.g., percent sand (USCS)).

Table 2.4. *General Sizing terms for USDA and USCS Classifications*

Particle Size	**USCS Classification**	**USDA Classification**
Large	Gravel	Sand
Medium	Sand	Silt
Small	Fines	Clay

Correlation and Regression

Correlation analysis is the process in which variable relationships are assessed. In this case, the independent variables are the topographic characteristics while the dependent variables are the soil textures. Correlation analysis relies on covariance-- the variables being related in some way (Reid, 2014). Pearson *r* is a commonly used form of correlation that assumes a linear relationship and quantifies the strength of that linear relationship with variable *r*, which ranges from -1 to 1 indicating a positive or negative correlation. The significance (α) of *r* is the magnitude of Type 1 error rate, which is the probability that the null hypothesis (there is no correlation) was incorrectly rejected and thus correlation was mistakenly assumed. While the choice of α is somewhat arbitrary, 0.05 is a commonly accepted

standard, indicating the null hypothesis is erroneously rejected 5% of the time. Regression expresses the relationship in the form of an equation, outputting a regression line (form Y' = bX+a with Y' representing the predicted value) (Reid, 2014). The square of correlation (r^2), defined as the coefficient of determination, measures the proportion of variance in one variable that is accounted for in another variable. For example, given a 0.2 coefficient of determination, knowing a given topographic characteristic accounts for 20% of the variability away from the mean of the corresponding soil texture. In this case, 80% of the variability of soil textures would not be accounted for and thus the relationship would not be strong. *P-values* measure the probability of getting a value at least as extreme as current data and are used in conjunction with the selected α. If the *p-value* is greater than α, the null hypothesis (there is no correlation) is accepted. If the *p-value* is less than α, the null hypothesis is rejected, and predictions of the dependent variable will be more accurate than the mean of the dependent variable regardless of the value of the independent variable. Together, *p-values* and coefficients of determination will give a measure of whether correlation exists and how well the regression accounts for variability. However, regression is a measure of association, not causation, meaning it is not a measure of cause and effect.

Variable predictability can be improved through the inclusion of multiple predictor variables (Reid, 2014). For instance, knowing both slope and elevation can improve the likelihood we can accurately predict particle size over only knowing slope. A common extension of linear regression that includes these additional variables is Multiple Linear Regression (MLR). MLRs expand on the linear regression equation to include these additional variables (form $Y' = b_1X_1 + b_2X_2 + b_0$), where each b value is defined as the regression weight for a given variable, also known as the slope. The intercept term (b_0) represents the value of the dependent variable when all dependent variables are equal to zero. In contrast, the regression coefficients (b_1, b_2, etc.) represent the change in the dependent variable that is expected for a unit change in each independent variable while holding all other independent variables constant (Reid, 2014). If the intercept term is significantly higher than any of the coefficients, it indicates that the baseline value of the dependent variable is relatively large compared to the effect of each independent variable. This may suggest that there are other factors beyond those indicated in the model that are driving the baseline value of the dependent variable. The relative magnitude of the intercept and regression coefficients can depend on the scale of the variables in the model; thus, each data series was standardized to remove the effect of large differences between the ranges of each variable. A second round of standardization was performed on each series of intercepts and coefficients for each dependent variable. Standardizing a data point includes subtracting the mean of the dataset

and dividing by the standard deviation of that dataset. This process scales the mean of a dataset to zero with a standard deviation of one. Simple linear regression, a form of MLR where all predictors are evaluated concurrently with any predictor not significantly enhancing the overall prediction being dropped, was used for this report. Like linear regression, there is not sufficient justification for concluding output is proof of causation but is sufficient for plausibility.

Results

Maxwell Ranch USDA Classification Output

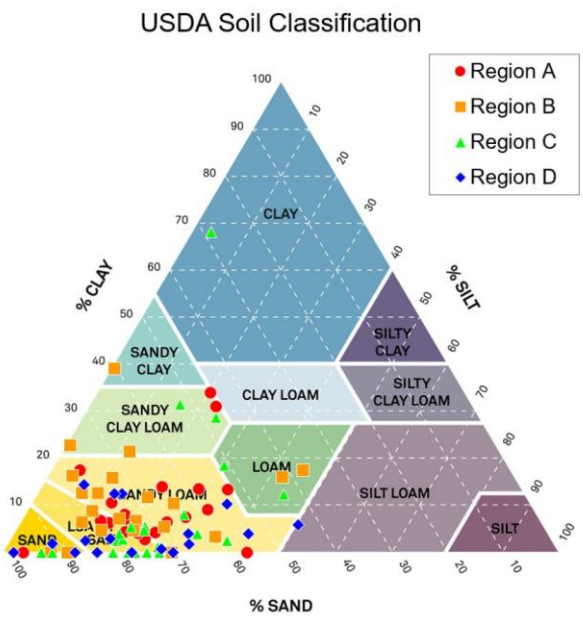

Fig. 2.1. *Maxwell Ranch USDA Soil Classification Output*

Linear Regressions

The simple linear regression analysis yielded correlation (*r*) and significance (*p*) values that indicate correlation strength and existence, respectively. Relationships where the null hypothesis is rejected (correlation exists) are considered for correlation strength via Pearson *r*, which considers negativity. This *r* ranges from -1 to 1 indicating a positive or negative correlation, with values closer to -1 or 1 being stronger fits. As there are no strictly defined categories of *r* outside these general rules, an

arbitrary scale is defined in Table (2.1) for simplicity. After each series of tables, significant regressions are displayed with their coefficients of determination (r^2).

Table 2.1. Absolute Value Strength of Regression Line Fit

|r|	Strength of Fit
$r < 0.3$	None
$0.3 < r < 0.5$	Weak
$0.5 < r < 0.7$	Moderate
$r > 0.7$	Strong

Ranch-wide analysis is considered first and captures all variability in the ranch, but, due to larger sample size, dampens the effect of unique sites on the regression and could lead to incorrect relationship inferences if analyzed alone. Regional analysis is conducted after, and, with regional samples being wholly representative of their respective regions, they better capture unique trends within those regions than the collective ranch-wide analysis. It is important to characterize these unique trends as they may not be captured in ranch-wide analysis. Relationships or the lack thereof from these regions are used in conjunction with ranch-wide results to analyze relationships across the topography of the ranch.

Color scales were arbitrarily chosen for better visibility of both strength and significance. Each *r* table (e.g., Table (2.2)) has a three-color scale with red at -0.5, yellow at 0, and green at 0.5. These values were chosen to better distinguish those relationships of moderate to strong correlation. Each *p-value* table (e.g., Table (2.3)) has a two-color scale of green at 0.05 and red at 0.06 to better display both relationships with significance and those bordering α. These scales are consistent across all regions.

Ranch-Wide Analysis

When considering the entirety of Maxwell Ranch, there are several noteworthy relationships as seen in Table (2.3). Their respective correlation strengths are seen in Table (2.2). The natural log of contributing area (Fig. 3.1) had a weak positive relationship with percent fines and percent clay and a weak negative relationship with percent gravel. This is expected, as smaller particles will be more impacted by the differential transport of grain sizes (smaller particles travel more readily than large particles) than larger particles. Some common causes of this transport are erosion, animal activity, wind, and drainage. The larger that area is, the more likely it is that smaller particles will travel down the

slope. Slope (Fig. 3.2) had a weak to moderate positive relationship with particle percentiles and percent gravel and a weak to moderate negative relationship with percent fines. These are expected, as the steeper a slope is, the more likely the fines will transport, leaving larger grain sizes behind. Elevation (Fig. 3.3) was weakly negatively correlated with hydraulic conductivity. This could be from more wind gusts present at higher elevation, moving smaller particles that would impede the transport of water. Northness (Fig. 3.4) was weakly negatively correlated with percent sand. Summer sun exposure (Fig. 3.5) had a weak to moderate negative correlation with particle percentiles and percent gravel and a weak positive correlation percent sand and percent fines. Both Northness and summer exposure are expected as sun exposure breaks down molecules in organic matter and soil aggregates. Winter sun exposure, however, is only correlated with the 10th particle diameter percentile. A potential explanation for summer sun correlating with more percentiles and classifications while winter sun did not is temperature variability. Temperature influences several soil and vegetative properties (e.g., physical weathering, soil organism activity, and changes in rate of chemical reactions in the soil) with high variability in temperature affecting soil structure and composition. Temperature generally fluctuates more in summer months than in winter, and this could explain the existing correlation between summer sun exposure and the lack of correlation with winter sun exposure. Vegetation (Figs. 3.6, 3.7, 3.8, 3.9, 3.10) had a weak to moderate positive relationship with percent fines, percent clay, and porosity, and weak negative relationships with percent sand and hydraulic conductivity. These are expected as larger particles are less likely to provide stability for vegetation to grow and vegetation somewhat negates particle movement. Vegetation is often connected with soil stability (e.g., trees preventing landslides), specifically in that grasses retain smaller particle sizes well, and the retention of those small particles will result in greater porosity. However, a common clay side-effect is poorly connected or clogged pores that limit water movement and is seen in Table (2.3) in the negatively correlated hydraulic conductivity.

Table 2.2. Ranch-Wide *Linear Regression Strength of Correlation (r) Values*

Ranch-wide: r	ln(CA)	Slope	Elevation	ln(aspect)	S*Cos(A)	S*Sin(A)	Curvature	S2 PSRI SS	S2 PSRI WS	S2 NDVI 05262022	S2 NDVI 06152022	LS NDVI 06142022	PCS NDVI 06132022	PCS NDVI 08062022
D10	-0.064	0.284	-0.129	0.068	0.140	-0.205	0.024	-0.338	0.220	-0.184	-0.114	-0.096	-0.183	-0.134
D30	-0.138	0.376	-0.029	-0.120	0.204	0.102	-0.049	-0.421	-0.060	-0.022	0.035	0.030	-0.022	0.041
D50	-0.181	0.402	0.064	-0.073	0.181	0.111	-0.111	-0.409	0.005	-0.077	-0.025	0.009	-0.078	0.009
D60	-0.187	0.394	0.101	-0.043	0.171	0.113	-0.121	-0.383	0.034	-0.106	-0.048	0.003	-0.096	-0.004
D90	-0.187	0.394	0.101	-0.043	0.171	0.113	-0.121	-0.383	0.034	-0.106	-0.048	0.003	-0.096	-0.004
D90-10	-0.246	0.443	0.132	0.019	0.151	0.017	-0.137	-0.402	0.023	-0.150	-0.087	0.034	-0.074	-0.012
% Gravel (USCS)	-0.215	0.415	0.042	0.040	0.104	0.005	-0.121	-0.407	0.117	-0.205	-0.133	-0.023	-0.183	-0.095
% Sand (USCS)	-0.039	-0.175	-0.137	-0.002	-0.252	0.037	0.072	0.246	-0.076	0.132	0.135	0.031	0.140	0.067
% Fines (USCS)	0.351	-0.412	-0.033	-0.025	0.109	-0.001	0.192	0.350	-0.063	0.215	0.149	0.058	0.183	0.103
% Sand (USDA)	-0.160	0.146	-0.189	0.056	-0.046	0.019	-0.188	-0.118	0.049	-0.305	-0.208	-0.176	-0.199	-0.198
% Silt (USDA)	-0.043	-0.106	0.054	-0.109	0.035	0.033	0.054	0.095	-0.053	-0.041	-0.115	-0.140	-0.094	-0.122
% Clay (USDA)	0.250	-0.077	0.186	0.042	0.022	-0.059	0.185	0.052	-0.007	0.435	0.388	0.374	0.355	0.383
Porosity	0.122	-0.146	0.170	-0.072	0.046	-0.008	0.169	0.120	-0.053	0.243	0.145	0.113	0.142	0.135
Ks [mm/d]	-0.184	0.144	-0.225	0.067	-0.006	0.018	-0.180	-0.117	0.075	-0.369	-0.255	-0.243	-0.254	-0.258

Table 2.3. *Ranch-Wide Linear Regression Significance (p) Values*

Ranch-wide: p-values	ln(CA)	Slope	Elevation	ln(aspect)	S*Cos(A)	S*Sin(A)	Curvature	S2 PSRI SS	S2 PSRI WS	S2 NDVI 05262022	S2 NDVI 06152022	LS NDVI 06142022	PCS NDVI 06132022	PCS NDVI 08062022
D10	0.557	0.007	0.231	0.527	0.193	0.055	0.825	0.001	0.040	0.086	0.289	0.373	0.088	0.212
D30	0.199	0.000	0.788	0.265	0.057	0.343	0.650	0.000	0.577	0.840	0.743	0.783	0.836	0.704
D50	0.091	0.000	0.556	0.500	0.091	0.304	0.304	0.000	0.961	0.474	0.820	0.932	0.468	0.933
D60	0.081	0.000	0.350	0.694	0.111	0.296	0.263	0.000	0.750	0.327	0.657	0.980	0.373	0.971
D90	0.081	0.000	0.350	0.694	0.111	0.296	0.263	0.000	0.750	0.327	0.657	0.980	0.373	0.971
D90-10	0.021	0.000	0.221	0.858	0.160	0.877	0.204	0.000	0.832	0.164	0.419	0.756	0.493	0.915
% Gravel (USCS)	0.045	0.000	0.701	0.715	0.336	0.963	0.261	0.000	0.277	0.055	0.216	0.829	0.089	0.377
% Sand (USCS)	0.721	0.104	0.203	0.988	0.018	0.736	0.503	0.021	0.481	0.220	0.211	0.772	0.194	0.534
% Fines (USCS)	0.001	0.000	0.757	0.817	0.312	0.996	0.074	0.001	0.558	0.044	0.166	0.589	0.087	0.338
% Sand (USDA)	0.137	0.175	0.077	0.605	0.673	0.861	0.079	0.275	0.653	0.004	0.052	0.101	0.063	0.064
% Silt (USDA)	0.692	0.324	0.616	0.313	0.749	0.760	0.618	0.377	0.622	0.702	0.287	0.192	0.384	0.257
% Clay (USDA)	0.019	0.477	0.083	0.695	0.840	0.587	0.084	0.633	0.950	0.000	0.000	0.000	0.001	0.000
Porosity	0.257	0.174	0.113	0.503	0.670	0.942	0.116	0.265	0.625	0.023	0.177	0.297	0.186	0.209
Ks [mm/d]	0.086	0.182	0.035	0.534	0.959	0.871	0.094	0.279	0.486	0.000	0.016	0.023	0.017	0.015

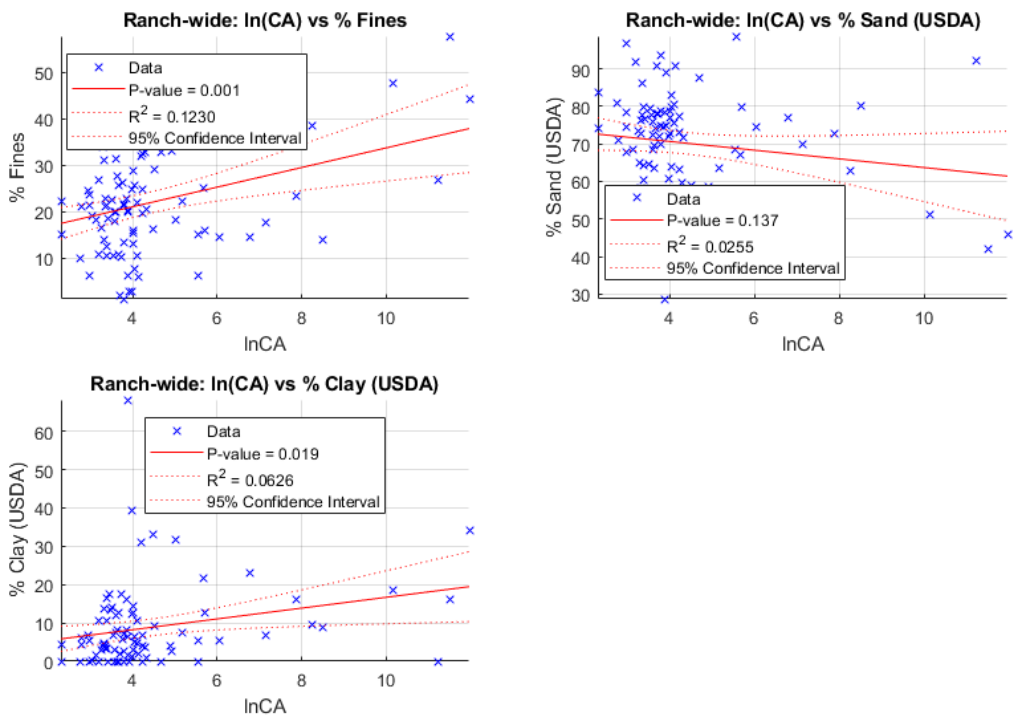

Fig. 3.1. *Natural Log of Contributing Area Regression Curves*

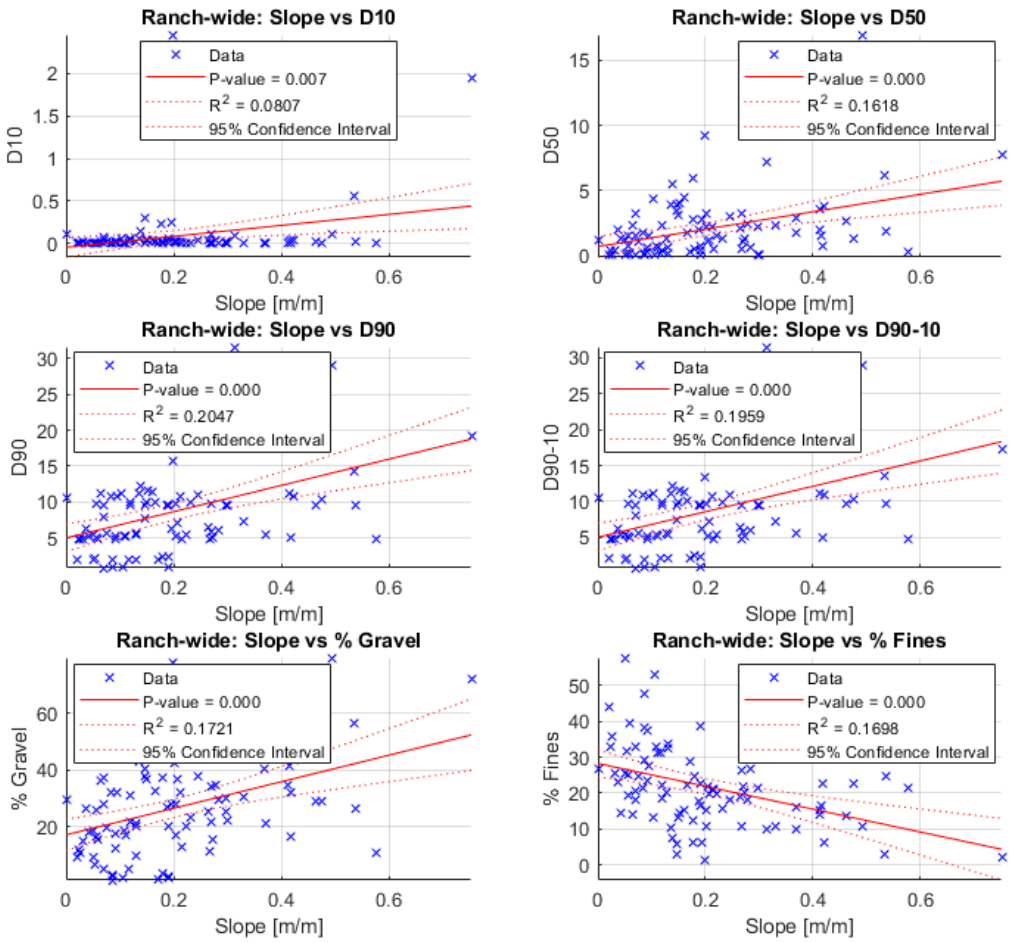

Fig. 3.2. *Slope Regression Curves*

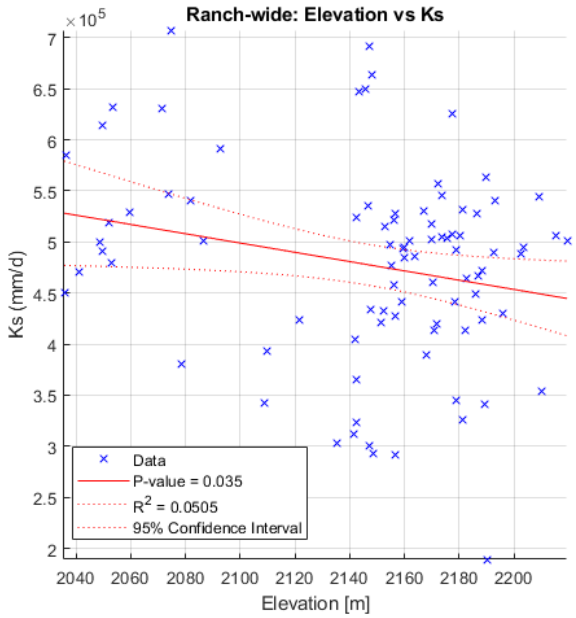

Fig. 3.3. *Elevation Regression Curve*

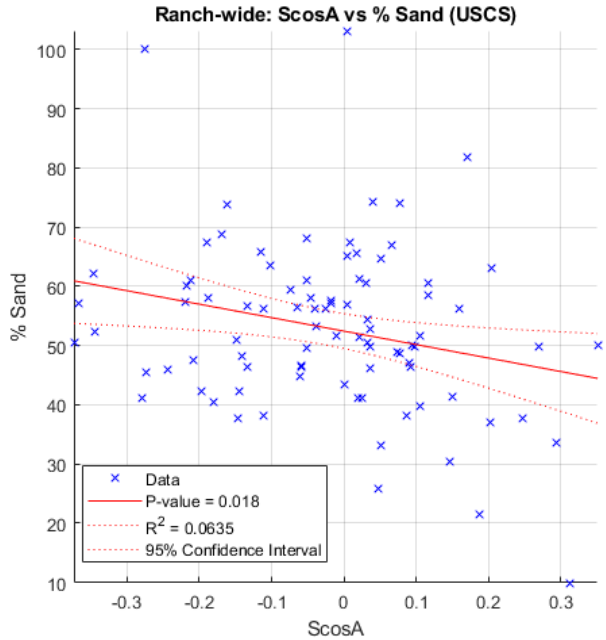

Fig. 3.4. *Northness Regression Curve*

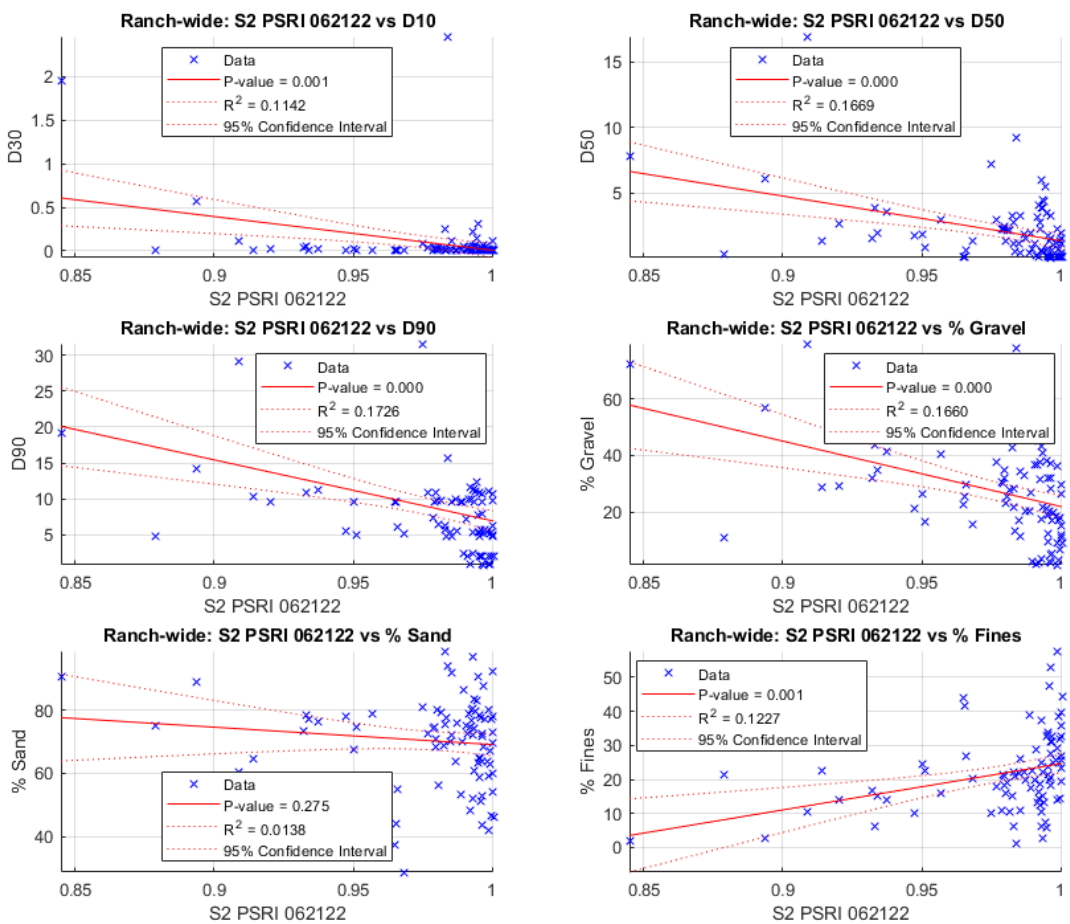

Fig. 3.5. *S2 PSRI Summer Solstice (06/21/2022) Regression Curves*

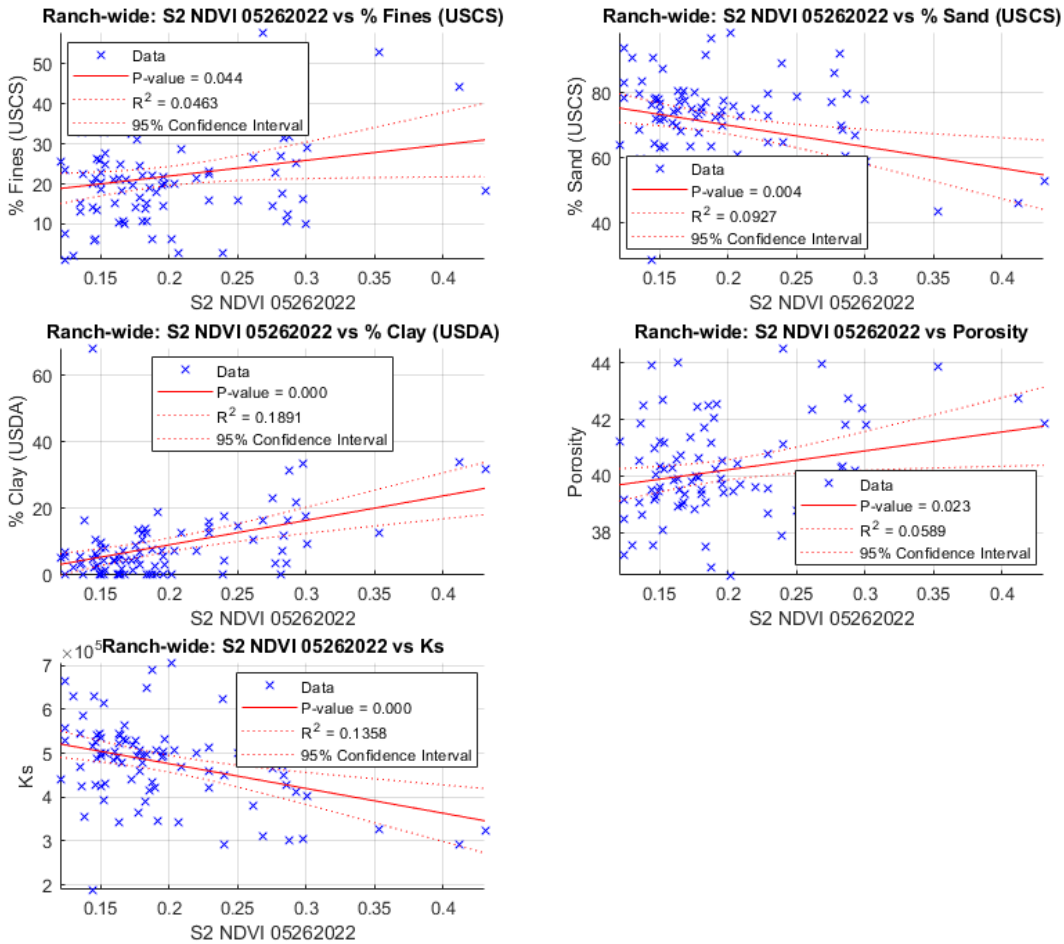

Fig. 3.6. *S2 NDVI 05/26/2022 Regression Curves*

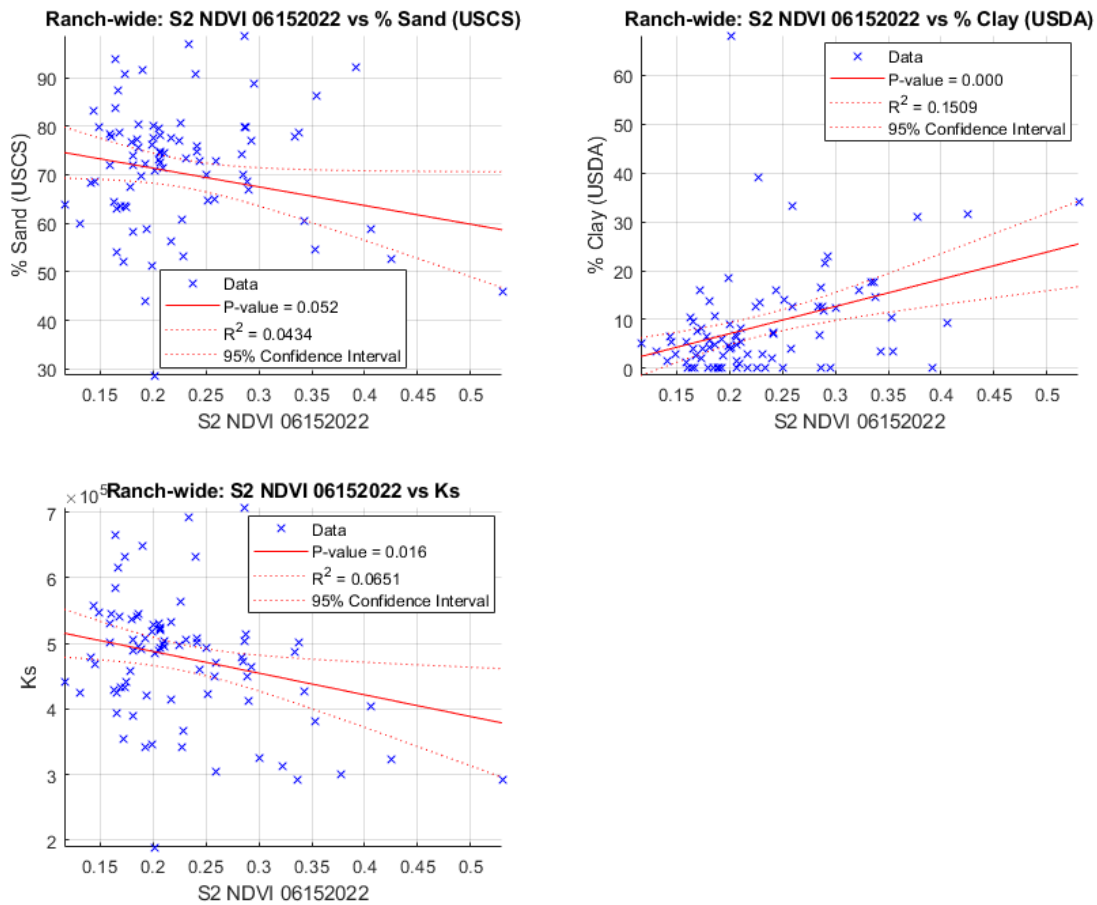

Fig. 3.7. *S2 NDVI 06/15/2022 Regression Curves*

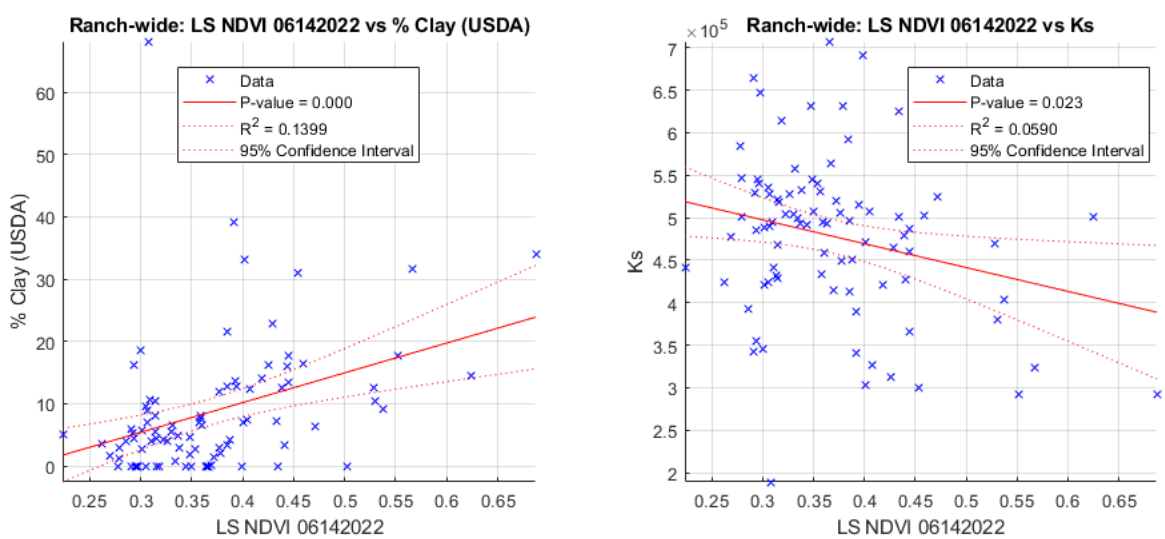

Fig. 3.8. *LS NDVI 06/14/2022 Regression Curves*

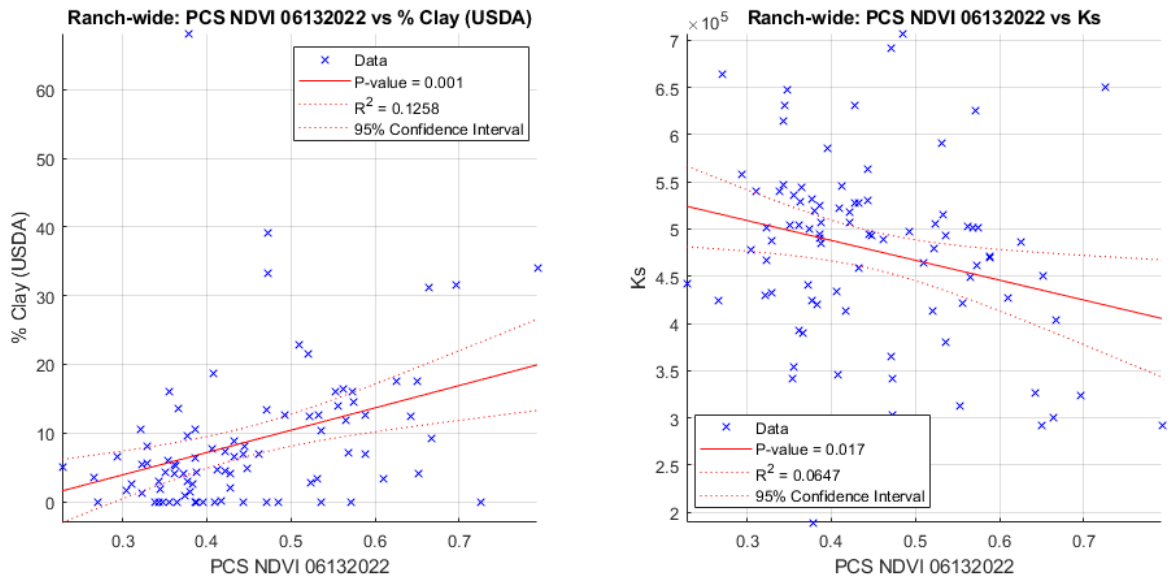

Fig. 3.9. *PCS NDVI 06/13/2022 Regression Curves*

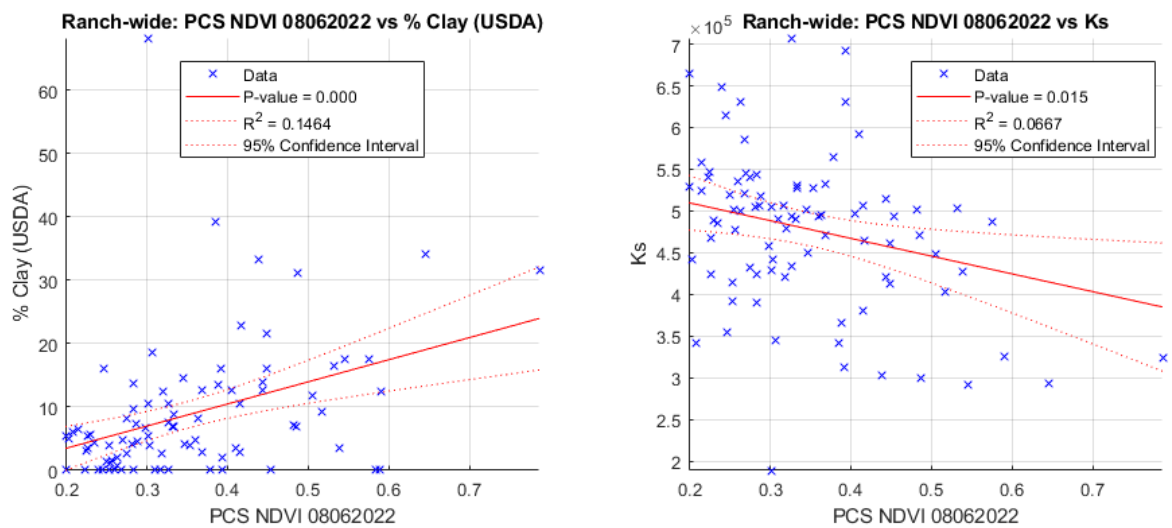

Fig. 3.10. *PCS NDVI 08/06/2022 Regression Curves*

Region A

Region A was the most topographically variable region on the ranch, containing sites seemingly consistent in soil types as the other regions, but contains many grassy areas including several sites in thick, marshy grasses. Table (2.5) shows that many of this region's textures were correlated with vegetation and contributing area while having little to no correlation with other variables. Table (2.4) expands on the strength of these relationships. The natural log of contributing area (Fig. 4.1) was weak to moderately negatively correlated with particle size percentiles, percent gravel, percent sand, and

hydraulic conductivity, and moderately to strongly positively correlated with percent fines and percent clay. This is expected, as larger particles are less likely to travel, and smaller particles are more likely to travel via the differential transport of grain size effect. As such, smaller particles are more likely to be present when the contributing area is larger. This same effect explains the particle percentiles because with a larger contributing area, a greater percentage of smaller particles are expected. As seen in the ranch-wide analysis, when there are more small particles present in the soil, the hydraulic conductivity is expected to drop due to clogging or poorly connected pores. Curvature has a moderately strong positive relationship with percent fines, but from Fig (4.2) there are too many outliers to confidently say there is a real relationship there. Vegetation (Figs. 4.3, 4.4, 4.5, 4.6, 4.7) was the most well-correlated, having moderate to strongly negative relationships with particle size percentiles, percent gravel, percent sand (USDA), and hydraulic conductivity, and strong positive relationships with percent fines and percent clay. It is expected that grasses will retain smaller particle sizes, which will in turn fill void spaces in larger particles, thus lowering the hydraulic conductivity, but having such strong negative relationships with larger particles and particle percentiles seems to indicate that there is a direct connection between grassy vegetation and particle size retained. Speculating about the lack of relationship to summer sun exposure, the presence of grasses could provide the soil with somewhat of a cover, insulating the soil from temperature variations to some degree.

Table 2.4 *Region A Linear Regression strength of correlation (r) values*

Site A: r	ln(CA)	Slope	Elevation	ln(aspect)	S*Cos(A)	S*Sin(A)	Curvature	S2 PSRI SS	S2 PSRI WS	S2 NDVI 05262022	S2 NDVI 06152022	LS NDVI 06142022	PCS NDVI 06132022	PCS NDVI 08062022
D10	-0.221	-0.093	-0.101	0.176	0.238	0.001	-0.100	0.154	0.139	-0.232	-0.180	-0.120	-0.201	-0.168
D30	-0.361	-0.021	-0.068	0.403	0.125	0.049	-0.281	0.075	0.195	-0.386	-0.335	-0.272	-0.448	-0.397
D50	-0.420	0.080	-0.115	0.414	0.026	-0.008	-0.228	0.022	0.300	-0.517	-0.487	-0.413	-0.581	-0.549
D60	-0.444	0.092	-0.111	0.391	-0.002	0.021	-0.211	0.025	0.297	-0.559	-0.536	-0.462	-0.608	-0.565
D90	-0.444	0.092	-0.111	0.391	-0.002	0.021	-0.211	0.025	0.297	-0.559	-0.536	-0.462	-0.608	-0.565
D90-10	-0.449	0.234	0.132	0.090	-0.211	-0.021	-0.185	-0.148	0.058	-0.582	-0.557	-0.460	-0.500	-0.434
% Gravel (USCS)	-0.437	0.171	-0.059	0.380	-0.119	-0.013	-0.190	-0.059	0.303	-0.637	-0.625	-0.521	-0.676	-0.627
% Sand (USCS)	0.078	0.103	0.336	-0.377	0.064	-0.029	-0.185	-0.183	-0.414	0.423	0.416	0.263	0.487	0.483
% Fines (USCS)	0.606	-0.417	-0.209	-0.176	0.142	0.016	0.533	0.348	-0.067	0.568	0.576	0.530	0.557	0.492
% Sand (USDA)	-0.478	0.358	0.279	0.173	-0.099	-0.084	-0.398	-0.253	0.108	-0.522	-0.500	-0.491	-0.433	-0.299
% Silt (USDA)	-0.026	-0.121	-0.068	-0.243	-0.135	-0.181	0.313	0.145	0.115	-0.057	-0.055	0.007	-0.106	-0.247
% Clay (USDA)	0.699	-0.376	-0.319	0.017	0.284	0.310	0.228	0.203	-0.272	0.794	0.760	0.682	0.720	0.681
Porosity	0.391	-0.325	-0.247	-0.198	0.053	0.029	0.400	0.242	-0.064	0.422	0.404	0.410	0.337	0.194
Ks [mm/d]	-0.517	0.314	0.265	0.156	-0.085	-0.136	-0.346	-0.195	0.169	-0.579	-0.539	-0.516	-0.485	-0.373

Table 2.5. *Region A Regression significance (p) values*

Site A: p-values	ln(CA)	Slope	Elevation	ln(aspect)	S*Cos(A)	S*Sin(A)	Curvature	S2 PSRI SS	S2 PSRI WS	S2 NDVI 05262022	S2 NDVI 06152022	LS NDVI 06142022	PCS NDVI 06132022	PCS NDVI 08062022
D10	0.348	0.695	0.671	0.458	0.312	0.996	0.675	0.518	0.558	0.325	0.447	0.615	0.395	0.478
D30	0.118	0.930	0.775	0.078	0.598	0.839	0.231	0.753	0.409	0.093	0.149	0.247	0.048	0.083
D50	0.065	0.738	0.629	0.069	0.912	0.973	0.334	0.926	0.199	0.019	0.029	0.070	0.007	0.012
D60	0.050	0.701	0.643	0.089	0.995	0.930	0.371	0.916	0.204	0.010	0.015	0.040	0.004	0.009
D90	0.050	0.701	0.643	0.089	0.995	0.930	0.371	0.916	0.204	0.010	0.015	0.040	0.004	0.009
D90-10	0.047	0.320	0.580	0.706	0.372	0.929	0.435	0.534	0.809	0.007	0.011	0.041	0.025	0.056
% Gravel (USCS)	0.054	0.471	0.805	0.098	0.618	0.957	0.422	0.805	0.193	0.003	0.003	0.018	0.001	0.003
% Sand (USCS)	0.744	0.665	0.148	0.102	0.790	0.902	0.435	0.441	0.069	0.063	0.068	0.262	0.029	0.031
% Fines (USCS)	0.005	0.067	0.377	0.458	0.549	0.945	0.016	0.133	0.778	0.009	0.008	0.016	0.011	0.028
% Sand (USDA)	0.033	0.121	0.234	0.466	0.676	0.726	0.082	0.281	0.651	0.018	0.025	0.028	0.056	0.200
% Silt (USDA)	0.913	0.610	0.775	0.301	0.572	0.444	0.179	0.541	0.630	0.811	0.819	0.978	0.657	0.294
% Clay (USDA)	0.001	0.102	0.170	0.943	0.226	0.183	0.333	0.390	0.245	0.000	0.000	0.001	0.000	0.001
Porosity	0.088	0.163	0.294	0.403	0.826	0.903	0.080	0.303	0.788	0.064	0.078	0.073	0.146	0.412
Ks [mm/d]	0.020	0.178	0.259	0.512	0.721	0.567	0.135	0.409	0.476	0.008	0.014	0.020	0.030	0.105

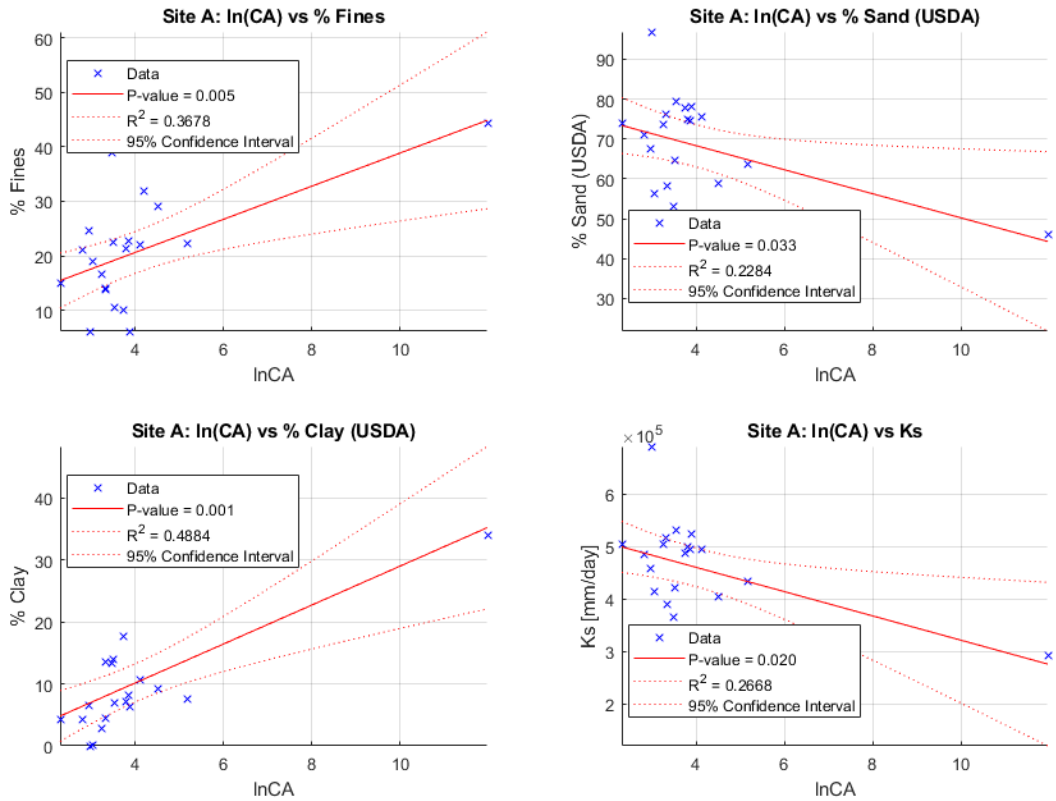

Fig. 4.1. *Natural Log of Contributing Area Regression Curves*

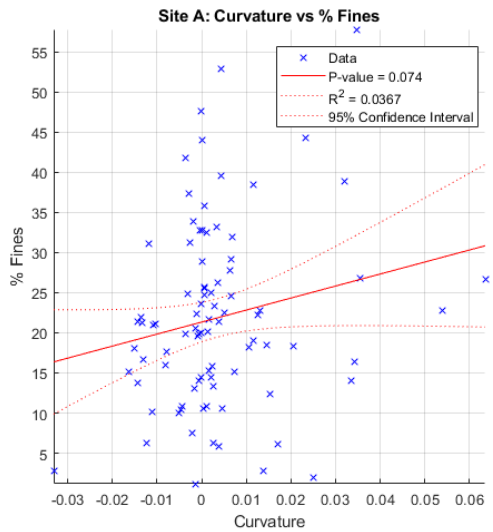

Fig. 4.2. *Curvature Regression Curve*

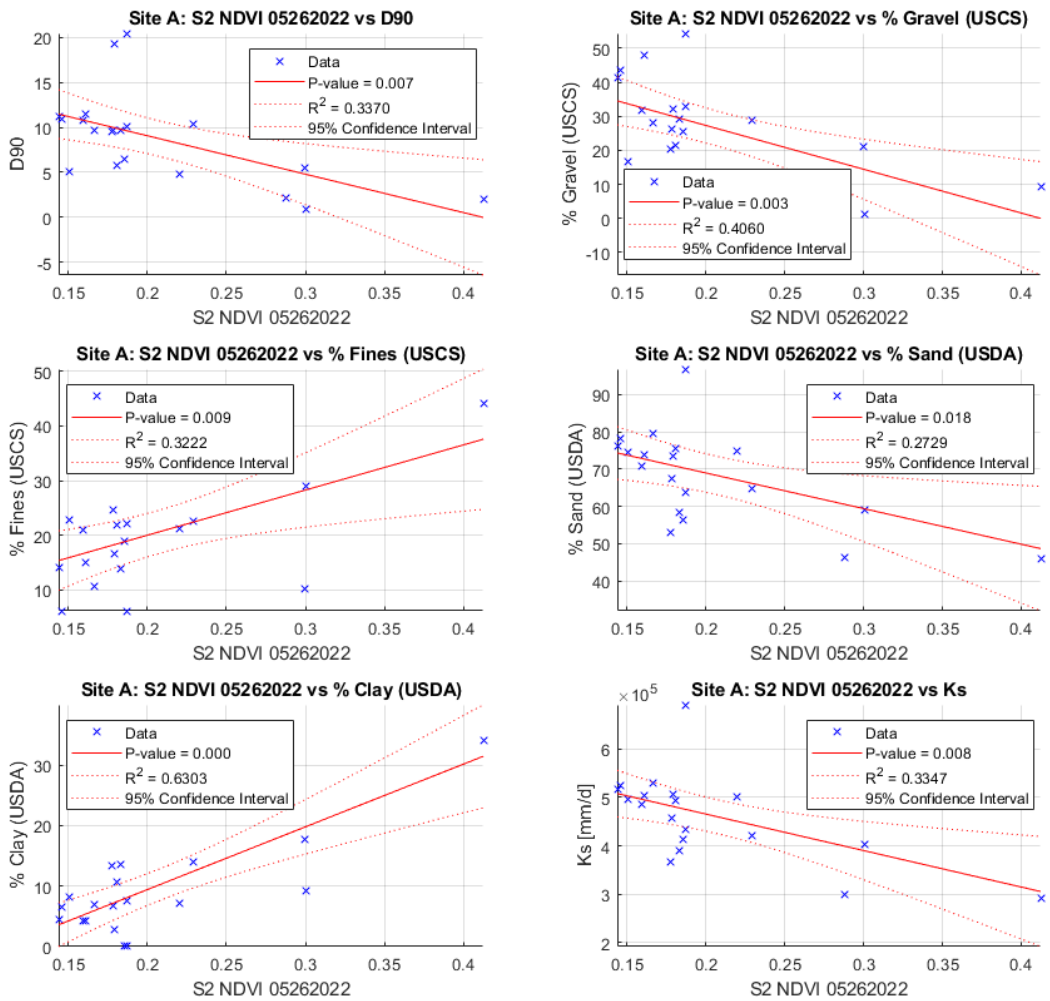

Fig. 4.3. *S2 NDVI 05/26/2022 Regression Curves*

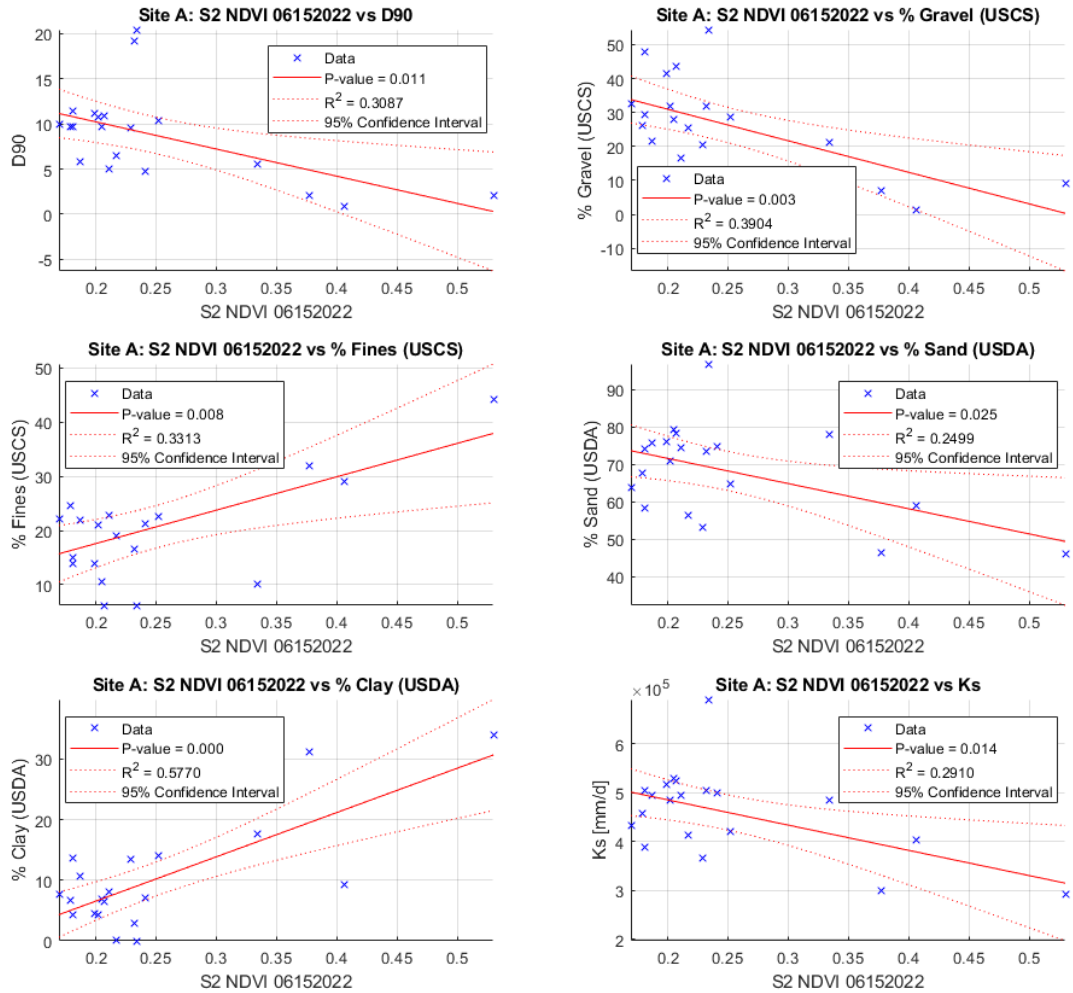

Fig. 4.4. *S2 NDVI 06/15/2022 Regression Curves*

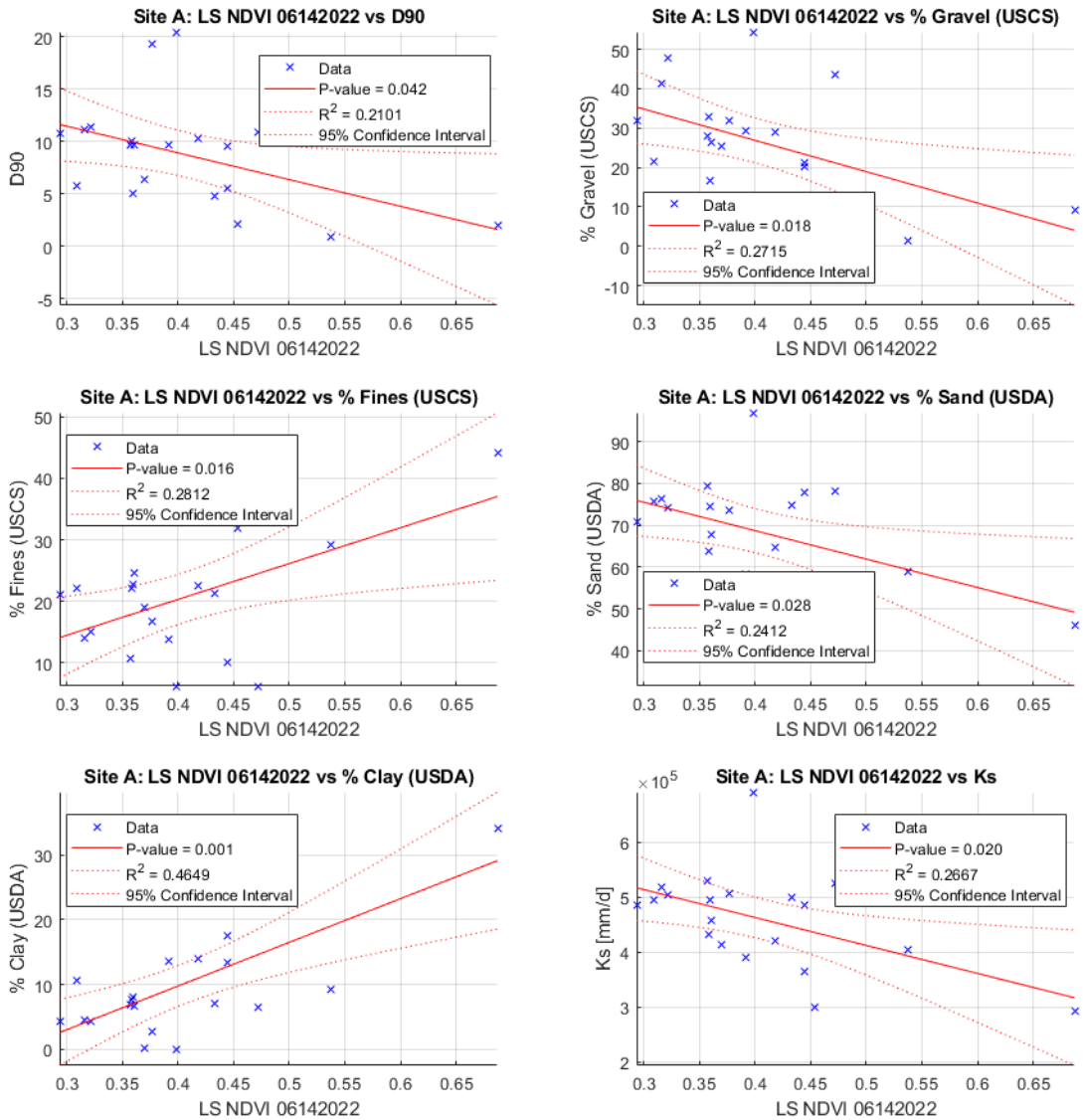

Fig. 4.5. *LS NDVI 06/14/2022 Regression Curves*

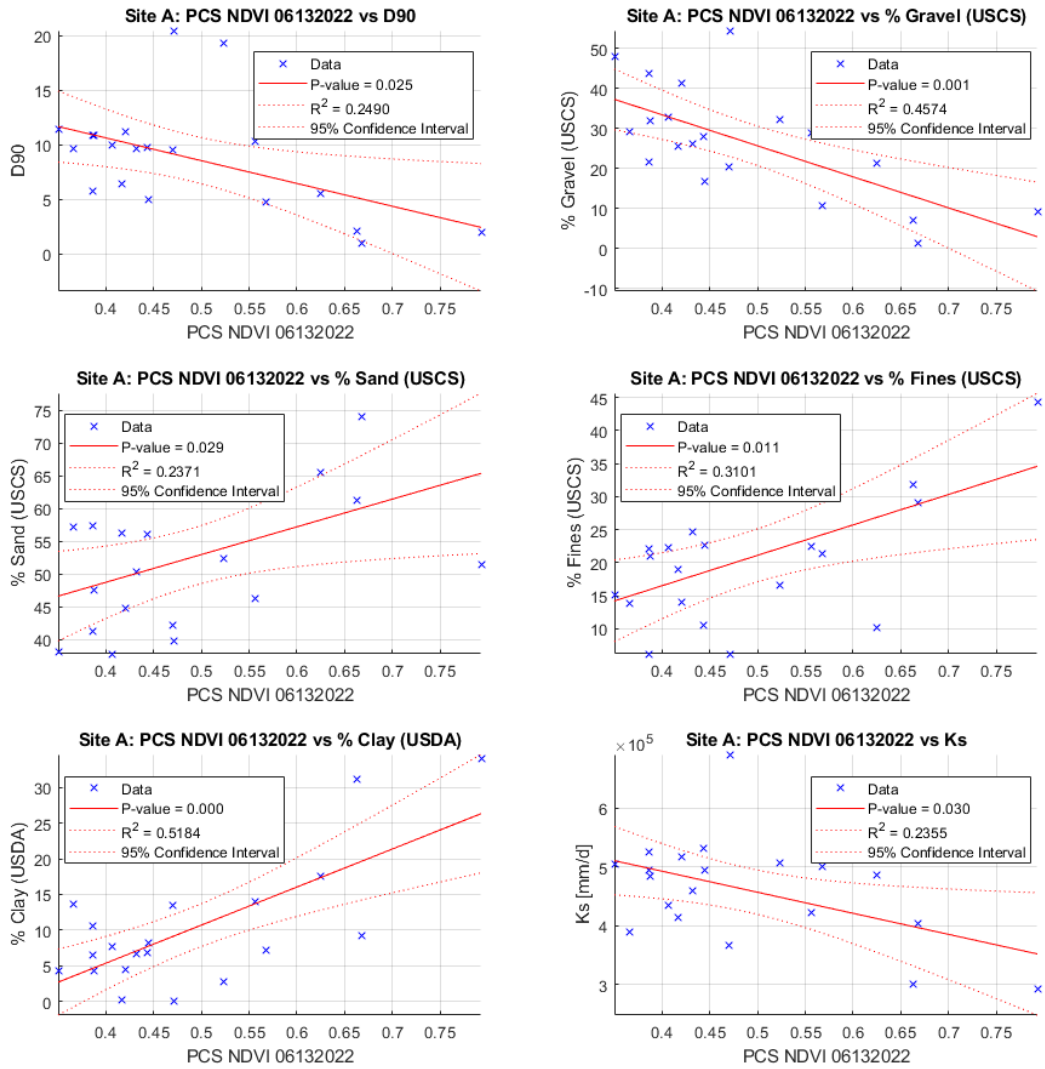

Fig. 4.6. *PCS NDVI 06/13/2022 Regression Curves*

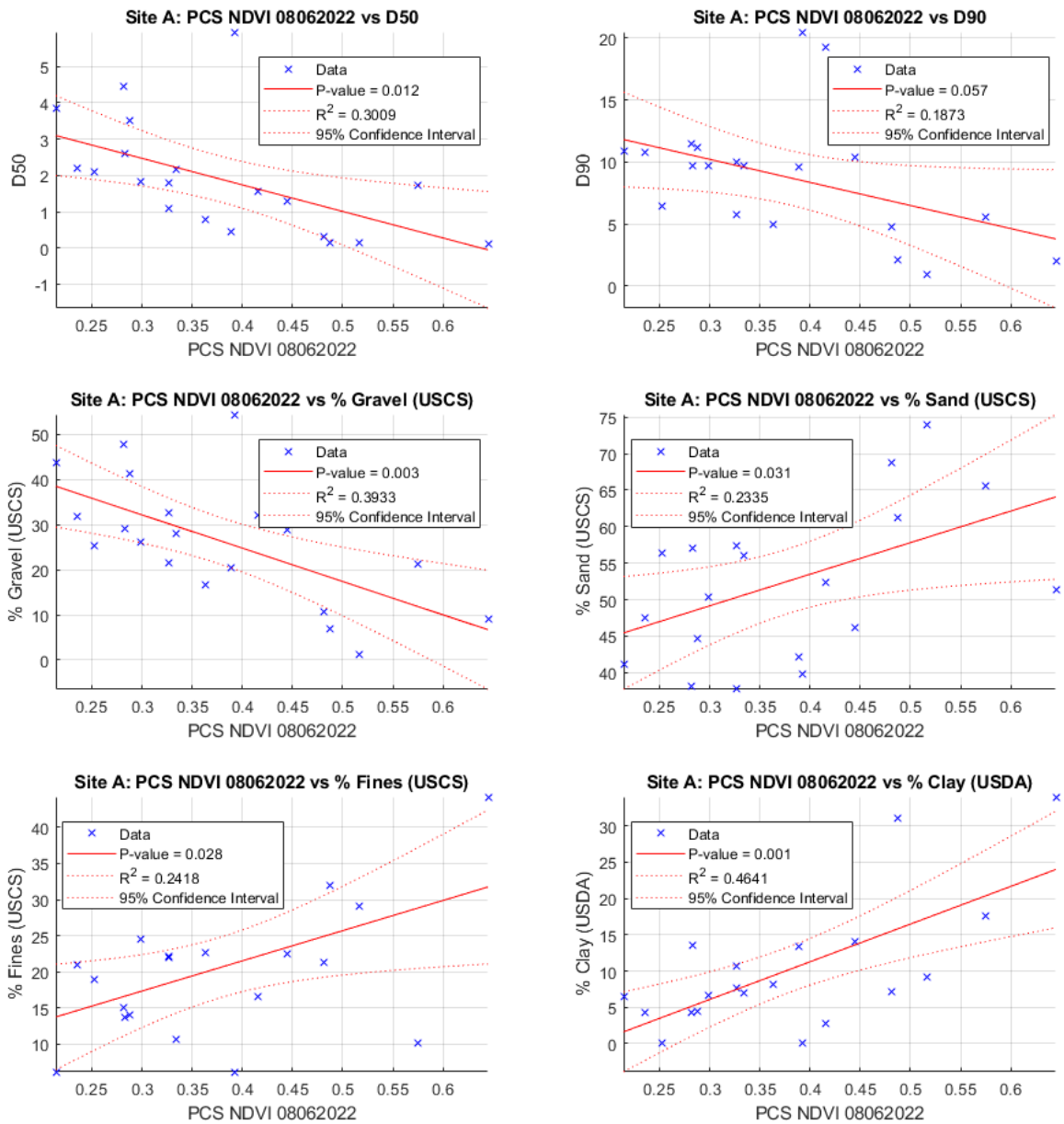

Fig. 4.7. *PCS NDVI 08/06/2022 Regression Curves*

Region B

Region B's vegetation was unique amongst the regions. While other regions consisted of mostly grasses or shrubs, region B consisted of mostly trees with sparse grasses. Table (2.7) shows the resulting significant relationships in such a unique area. Expanding on correlation strength, Table (2.6) shows several moderate to strong relationships. The natural log of contributing area (Fig. 5.1) was moderately

positively correlated with percent fines but doesn't have a significant relationship with hydraulic conductivity like other regions. Slope (Fig. 5.2) and Eastness (Fig. 5.5) were moderately to strongly correlated with particle diameter percentiles and percent gravel, and moderately negatively correlated with percent sand (USCS). It is expected that higher slopes tend to retain larger particles better than smaller particles due to differential transport of grain sizes. With Eastness being an indicator of wind exposure from the west, the expectation is that a greater percentage of smaller particles would exist on an east-facing slope. However, the wind in the region doesn't blow consistently out of a strictly eastern direction and few sites were on a purely eastern slope. This result is more expected of a west-facing slope and indicates the wind in the area may be heavily influenced by the deep ravines and cover it had from the west. Elevation (Fig. 5.3) was moderately positively correlated with percent fines as is expected at higher elevations that typically have less cover from the wind. Northness (Fig. 5.4) was moderately to strongly negatively correlated with percent sand (USCS). Summer sun exposure (Fig. 5.7) was strongly negatively correlated with particle diameter percentiles and percent gravel, and moderately positively correlated with percent sand (USCS). Both Northness and summer sun exposure results are expected as direct sunlight has an erosive effect on soils. Winter sun exposure (Fig. 5.8) only having moderately negative relationships with D10 and D30 indicate there are fewer smaller particles when more exposed. A potential explanation is that more winter sun exposure could cause snowmelt, transporting smaller particles and leaving larger particles. The lack of vegetation correlation is unique when considering other regions' strong vegetation relationships. Vegetation type may be the reason for the lack of correlation.

Table 2.6. *Region B Linear Regression strength of correlation (r) values*

Site B: r	ln(CA)	Slope	Elevation	ln(aspect)	S*Cos(A)	S*Sin(A)	Curvature	S2 PSRI SS	S2 PSRI WS	S2 NDVI 05262022	S2 NDVI 06152022	LS NDVI 06142022	PCS NDVI 06132022	PCS NDVI 08062022
D10	-0.108	0.556	-0.020	0.115	-0.165	0.744	-0.523	-0.675	-0.460	0.002	0.122	0.124	0.111	0.301
D30	-0.286	0.589	-0.137	-0.218	0.313	0.649	-0.135	-0.642	-0.463	0.123	0.164	0.096	0.095	0.181
D50	-0.303	0.592	-0.089	-0.204	0.253	0.664	-0.187	-0.643	-0.417	0.023	0.053	0.015	0.005	0.108
D60	-0.298	0.588	-0.067	-0.174	0.234	0.650	-0.197	-0.643	-0.382	-0.034	-0.005	-0.031	-0.037	0.077
D90	-0.298	0.588	-0.067	-0.174	0.234	0.650	-0.197	-0.643	-0.382	-0.034	-0.005	-0.031	-0.037	0.077
D90-10	-0.354	0.633	-0.158	0.087	0.373	0.415	-0.079	-0.628	-0.364	-0.116	-0.067	0.004	-0.043	0.090
% Gravel (USCS)	-0.349	0.592	-0.040	-0.047	0.178	0.636	-0.272	-0.633	-0.345	-0.228	-0.166	-0.080	-0.159	-0.007
% Sand (USCS)	0.005	-0.437	0.451	0.007	-0.517	-0.485	-0.150	0.524	0.362	-0.019	-0.198	-0.251	-0.144	-0.160
% Fines (USCS)	0.451	-0.328	-0.389	0.053	0.276	-0.339	0.493	0.296	0.083	0.322	0.413	0.353	0.354	0.174
% Sand (USDA)	0.019	-0.016	0.088	0.026	-0.332	0.225	-0.273	-0.034	-0.001	-0.153	-0.177	-0.238	-0.122	-0.043
% Silt (USDA)	-0.009	0.216	-0.190	-0.188	0.297	-0.029	0.107	-0.189	-0.197	0.019	0.168	0.137	0.135	0.058
% Clay (USDA)	-0.015	-0.274	0.135	0.222	0.068	-0.285	0.244	0.309	0.272	0.194	0.024	0.155	-0.009	-0.016
Porosity	-0.018	0.070	-0.120	-0.071	0.340	-0.184	0.243	-0.024	-0.051	0.125	0.184	0.223	0.132	0.049
Ks [mm/d]	0.066	0.082	-0.034	0.008	-0.288	0.302	-0.272	-0.146	-0.105	-0.168	-0.094	-0.169	-0.042	0.018

Table 2.7. *Region B Regression significance (p) values*

Site B: p-values	ln(CA)	Slope	Elevation	ln(aspect)	S*Cos(A)	S*Sin(A)	Curvature	S2 PSRI SS	S2 PSRI WS	S2 NDVI 05262022	S2 NDVI 06152022	LS NDVI 06142022	PCS NDVI 06132022	PCS NDVI 08062022
D10	0.634	0.007	0.930	0.611	0.462	0.000	0.013	0.001	0.031	0.994	0.589	0.584	0.622	0.174
D30	0.196	0.004	0.542	0.330	0.156	0.001	0.550	0.001	0.030	0.585	0.467	0.672	0.674	0.420
D50	0.171	0.004	0.694	0.362	0.257	0.001	0.404	0.001	0.054	0.919	0.816	0.946	0.982	0.632
D60	0.177	0.004	0.766	0.440	0.295	0.001	0.379	0.001	0.080	0.882	0.983	0.890	0.869	0.733
D90	0.177	0.004	0.766	0.440	0.295	0.001	0.379	0.001	0.080	0.882	0.983	0.890	0.869	0.733
D90-10	0.106	0.002	0.481	0.702	0.087	0.055	0.726	0.002	0.096	0.606	0.766	0.987	0.849	0.689
% Gravel (USCS)	0.111	0.004	0.859	0.836	0.428	0.001	0.221	0.002	0.116	0.307	0.461	0.725	0.479	0.975
% Sand (USCS)	0.984	0.042	0.035	0.977	0.014	0.022	0.504	0.012	0.098	0.932	0.378	0.260	0.524	0.476
% Fines (USCS)	0.035	0.137	0.074	0.814	0.214	0.123	0.020	0.181	0.712	0.144	0.056	0.107	0.106	0.439
% Sand (USDA)	0.932	0.945	0.696	0.907	0.132	0.314	0.219	0.881	0.997	0.498	0.429	0.286	0.588	0.848
% Silt (USDA)	0.969	0.334	0.397	0.401	0.179	0.899	0.634	0.398	0.380	0.934	0.454	0.542	0.548	0.798
% Clay (USDA)	0.947	0.217	0.551	0.320	0.765	0.198	0.274	0.162	0.221	0.387	0.914	0.491	0.967	0.942
Porosity	0.938	0.758	0.595	0.754	0.122	0.412	0.275	0.917	0.821	0.580	0.412	0.318	0.560	0.828
Ks [mm/d]	0.770	0.716	0.879	0.972	0.194	0.172	0.221	0.517	0.642	0.456	0.676	0.453	0.853	0.937

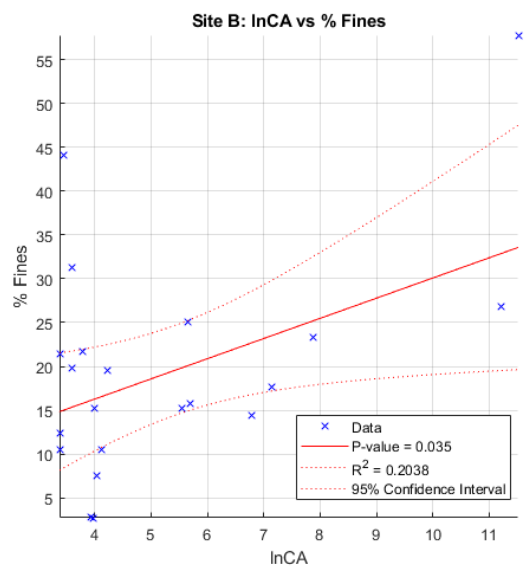

Fig. 5.1. *Contributing Area Regression Curve*

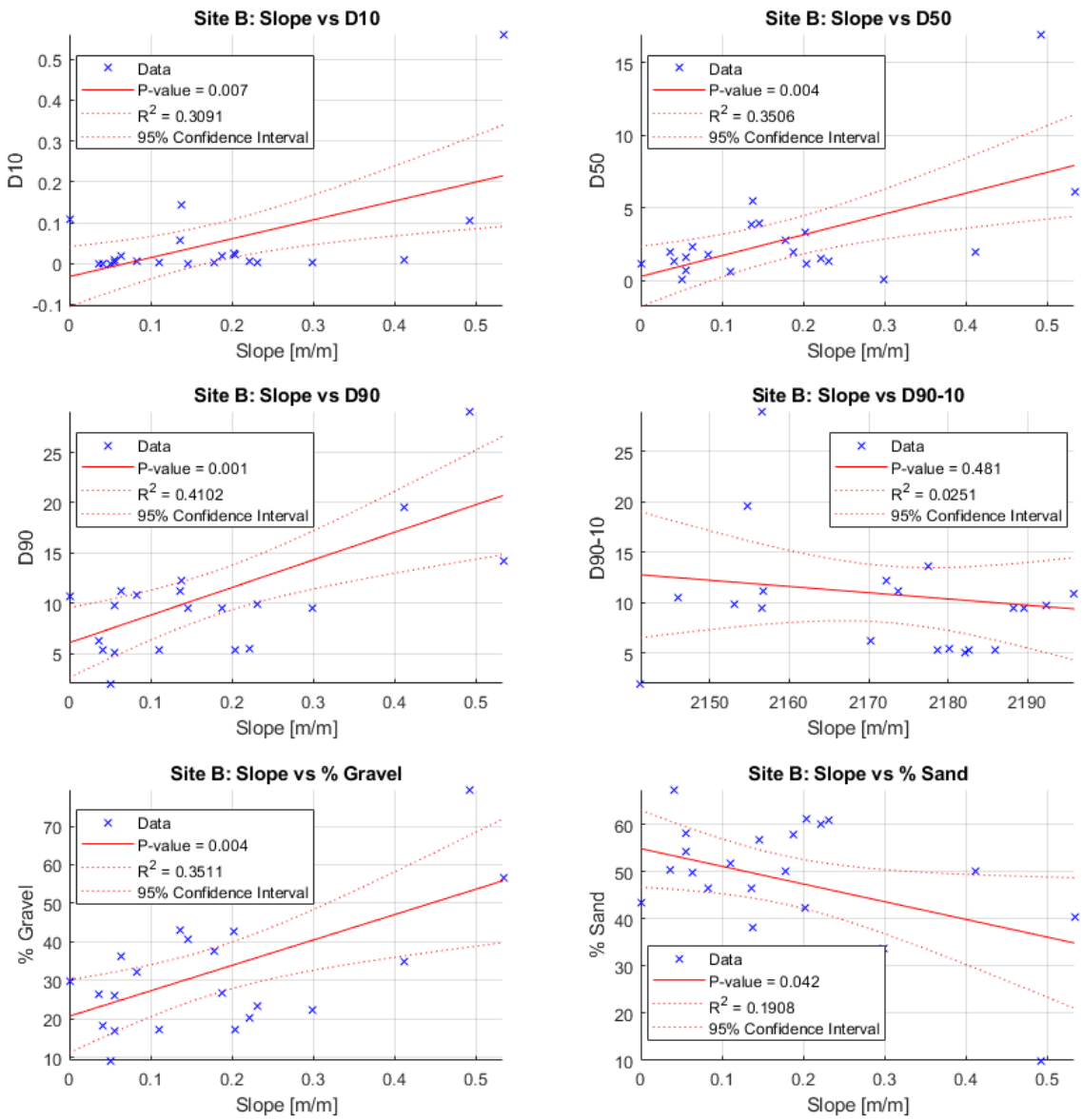

Fig. 5.2. *Slope Regression Curves*

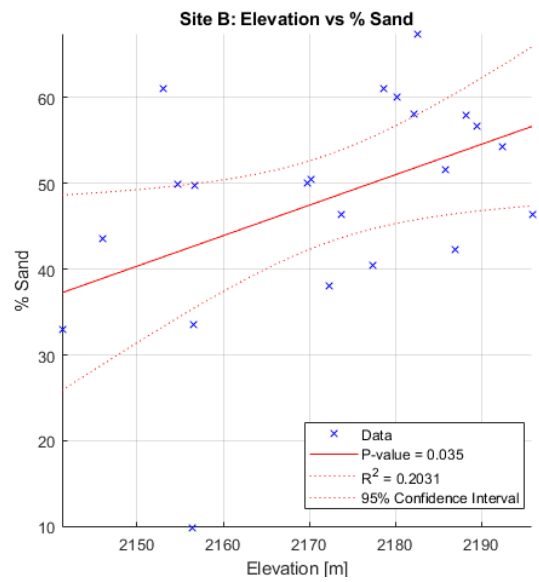

Fig. 5.3. *Elevation Regression Curve*

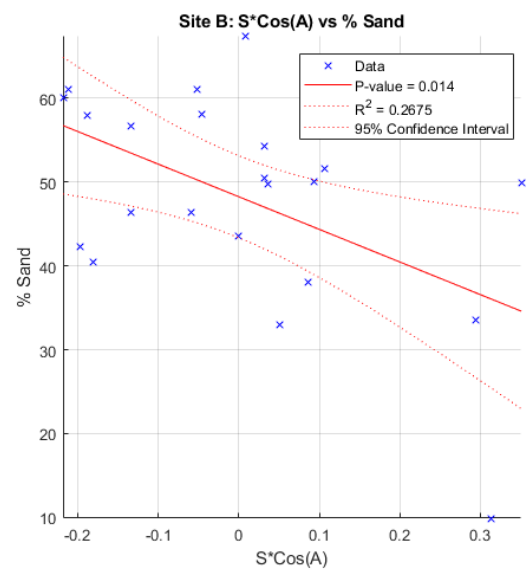

Fig. 5.4. *Northness Regression Curves*

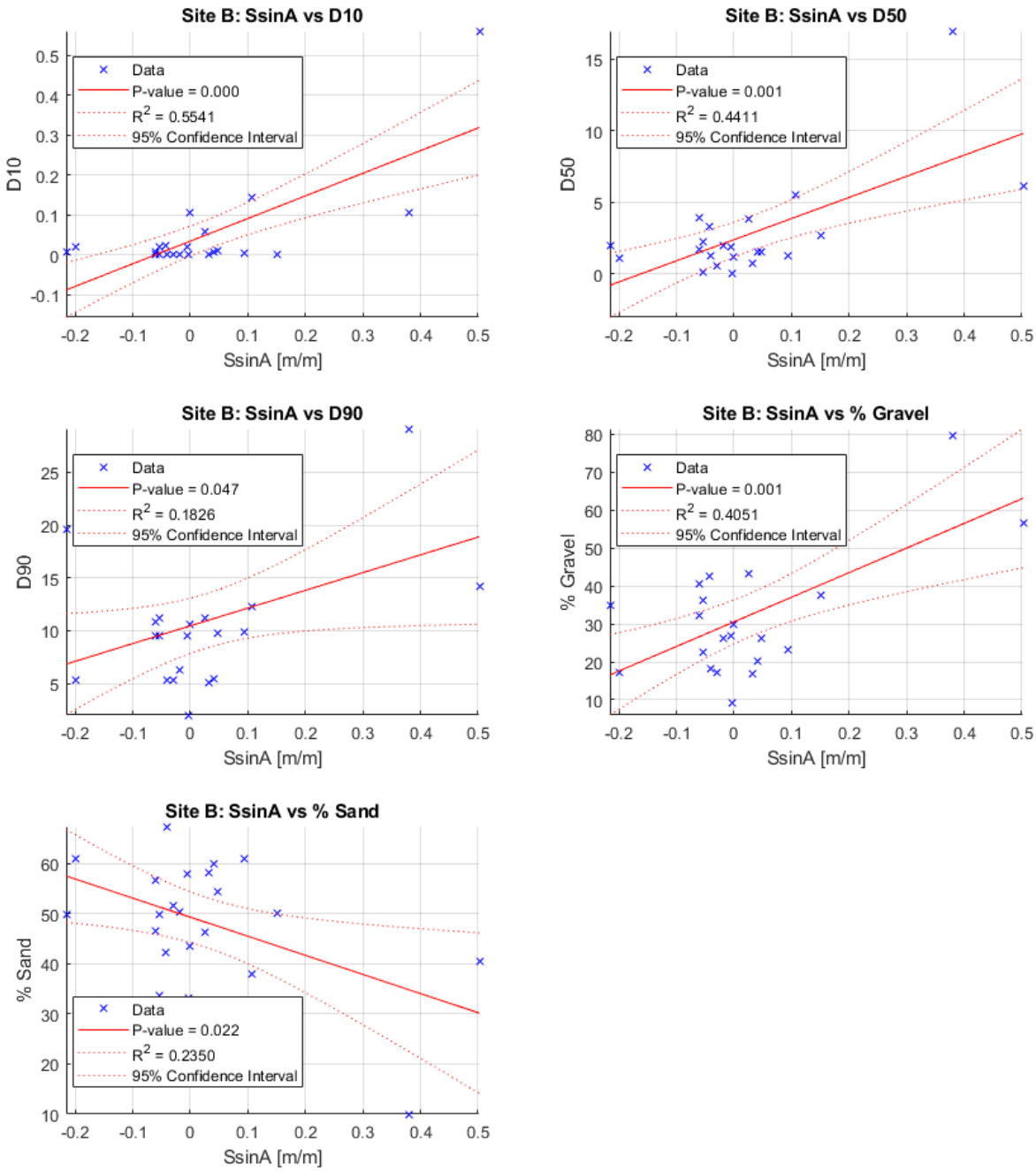

Fig. 5.5. *Eastness Regression Curves*

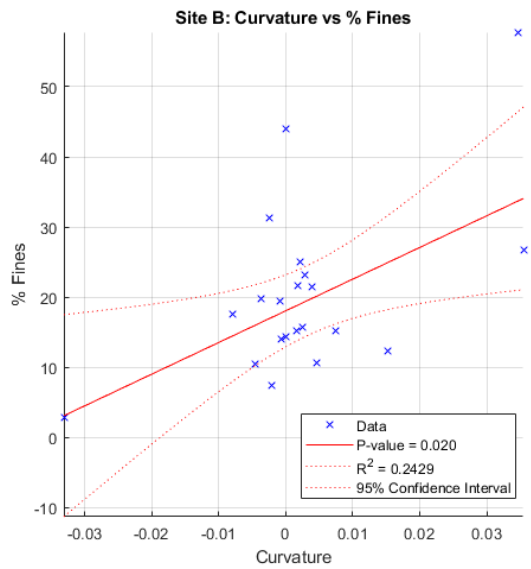

Fig. 5.6. *Curvature Regression Curve*

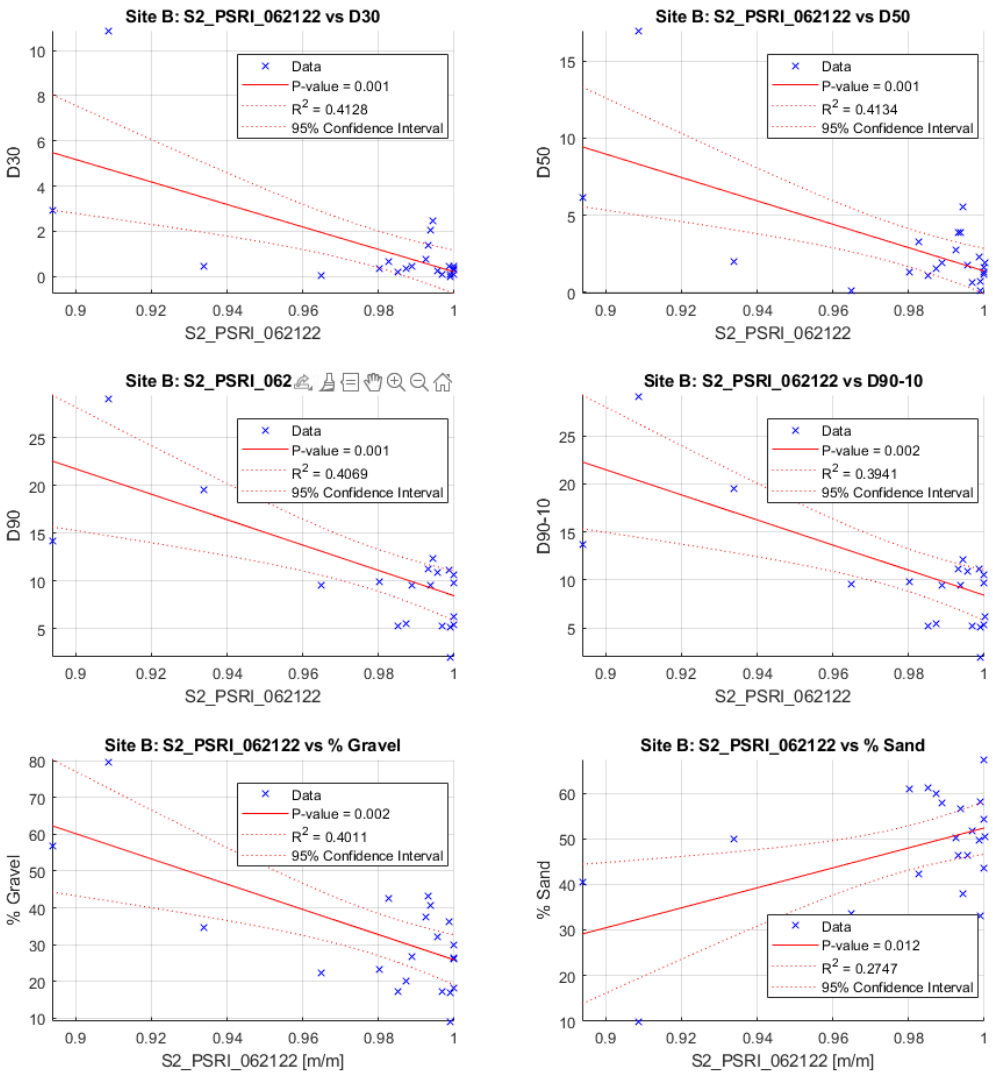

Fig. 5.7. *S2 PSRI Summer Solstice (06/21/2022) Regression Curves*

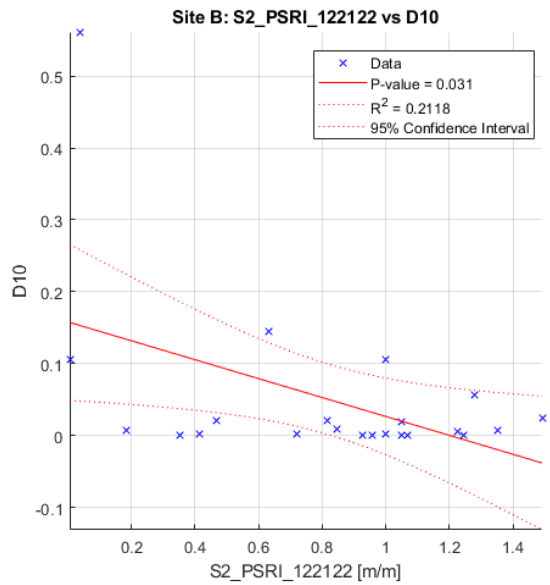

Fig. 5.8. *S2 PSRI Winter Solstice (12/21/2022) Regression Curves*

Region C

Region C was the windiest of the regions and the least protected by surrounding topography. The significant relationships of this region (Table 2.9) and their strengths (Table 2.8) give insight into this region where half the sites had minimal vegetation and the remaining sites were near grasses, shrubs, or sparsely spread trees.

The natural log of contributing area (Fig. 6.1) was moderately positively correlated with percent fines. Slope (Fig. 6.2) was moderately negatively correlated with percent fines. This is consistent with expectations as detailed for previous regions where smaller particles are more likely to travel when the contributing area is larger.

Eastness (Fig. 6.3) was strongly positively correlated with percent sand (USDA) and hydraulic conductivity, and moderately to strongly negatively correlated with percent clay and porosity. This is a series of interesting relationships, as the expectation for east-facing slopes is that they would have a greater percentage of smaller particles, and that porosity and hydraulic conductivity would be directly linked. However, like in region B, the correlations are acting like west-facing slopes in that fewer small particles are accumulating, and like other regions, increasing porosity does not cause increasing hydraulic conductivity. This suggests the wind didn't blow exclusively out of the west and that clays persist enough to disrupt the flow of water. Curvature (Fig. 6.4) is moderately negatively correlated with percent sand (USDA) and hydraulic conductivity, and moderately positively correlated with percent clay.

Summer sun exposure (Fig. 6.5) was moderately negatively correlated with higher particle size percentiles in D60, D90, effective particle range in D90-10, and moderately positively correlated with percent fines and percent silt. Like other regions, direct sun exposure degrades soil particle size, and the effective range shrinks with the larger particles degrading. The higher temperature variability of summer can possibly explain the lack of correlation with winter sun exposure. Vegetation (Figs. 6.6, 6.7, 6.8, 6.9) was moderately negatively correlated with percent sand and hydraulic conductivity, and moderately positively correlated with porosity. This indicates enough smaller particles exist in the soil to disrupt water flow.

Table 2.8. *Region C Linear Regression strength of correlation (r) values*

Site C: r	ln(CA)	Slope	Elevation	ln(aspect)	S*Cos(A)	S*Sin(A)	Curvature	S2 PSRI SS	S2 PSRI WS	S2 NDVI 05262022	S2 NDVI 06152022	LS NDVI 06142022	PCS NDVI 06132022	PCS NDVI 08062022
D10	-0.073	0.101	-0.249	-0.076	0.234	-0.054	-0.071	-0.158	0.238	-0.224	-0.183	-0.176	-0.311	-0.254
D30	-0.078	0.154	-0.279	-0.079	0.224	0.035	-0.070	-0.210	0.274	-0.161	-0.096	-0.064	-0.279	-0.198
D50	-0.199	0.359	-0.188	-0.001	0.307	0.254	-0.130	-0.413	0.389	-0.158	-0.009	0.065	-0.199	-0.121
D60	-0.228	0.387	-0.126	0.015	0.335	0.294	-0.143	-0.435	0.406	-0.173	-0.008	0.072	-0.177	-0.106
D90	-0.228	0.387	-0.126	0.015	0.335	0.294	-0.143	-0.435	0.406	-0.173	-0.008	0.072	-0.177	-0.106
D90-10	-0.299	0.442	0.042	0.031	0.285	0.384	-0.208	-0.468	0.337	-0.230	-0.050	0.045	-0.151	-0.116
% Gravel (USCS)	-0.234	0.262	-0.194	-0.063	0.229	0.183	-0.136	-0.339	0.329	-0.197	-0.055	0.045	-0.265	-0.165
% Sand (USCS)	-0.020	-0.004	0.046	0.074	-0.186	-0.021	0.232	0.118	-0.333	0.145	0.071	0.038	0.150	0.122
% Fines (USCS)	0.450	-0.478	0.248	0.022	-0.186	-0.272	-0.020	0.466	-0.183	0.267	0.123	-0.010	0.374	0.248
% Sand (USDA)	-0.384	0.200	-0.046	-0.126	0.099	0.614	-0.424	-0.022	-0.196	-0.486	-0.445	-0.346	-0.515	-0.485
% Silt (USDA)	0.218	-0.416	0.157	0.024	-0.109	-0.007	-0.051	0.494	-0.253	0.209	0.029	-0.005	0.257	0.169
% Clay (USDA)	0.240	0.053	-0.046	0.106	-0.032	-0.588	0.436	-0.272	0.339	0.344	0.413	0.337	0.345	0.368
Porosity	0.401	-0.270	0.074	0.122	-0.114	-0.573	0.385	0.119	0.132	0.495	0.421	0.322	0.531	0.486
Ks [mm/d]	-0.400	0.209	-0.018	-0.140	0.106	0.618	-0.471	-0.037	-0.177	-0.514	-0.487	-0.401	-0.530	-0.517

Table 2.9. *Region C Regression significance (p) values*

Site C: p-values	ln(CA)	Slope	Elevation	ln(aspect)	S*Cos(A)	S*Sin(A)	Curvature	S2 PSRI SS	S2 PSRI WS	S2 NDVI 05262022	S2 NDVI 06152022	LS NDVI 06142022	PCS NDVI 06132022	PCS NDVI 08062022
D10	0.748	0.653	0.263	0.736	0.295	0.810	0.755	0.481	0.287	0.316	0.415	0.433	0.159	0.253
D30	0.729	0.493	0.208	0.727	0.317	0.878	0.756	0.348	0.217	0.474	0.672	0.776	0.208	0.377
D50	0.376	0.101	0.402	0.998	0.164	0.255	0.563	0.056	0.074	0.482	0.968	0.775	0.375	0.590
D60	0.308	0.075	0.576	0.946	0.128	0.184	0.527	0.043	0.061	0.441	0.970	0.749	0.431	0.640
D90	0.308	0.075	0.576	0.946	0.128	0.184	0.527	0.043	0.061	0.441	0.970	0.749	0.431	0.640
D90-10	0.177	0.040	0.852	0.891	0.198	0.078	0.353	0.028	0.125	0.302	0.823	0.843	0.503	0.608
% Gravel (USCS)	0.296	0.238	0.387	0.781	0.305	0.415	0.545	0.123	0.134	0.380	0.809	0.844	0.234	0.464
% Sand (USCS)	0.931	0.985	0.840	0.744	0.408	0.926	0.300	0.601	0.130	0.519	0.754	0.867	0.507	0.588
% Fines (USCS)	0.036	0.024	0.265	0.924	0.408	0.221	0.929	0.029	0.415	0.229	0.586	0.965	0.087	0.267
% Sand (USDA)	0.078	0.371	0.837	0.578	0.660	0.002	0.049	0.924	0.382	0.022	0.038	0.114	0.014	0.022
% Silt (USDA)	0.330	0.054	0.486	0.915	0.629	0.977	0.821	0.019	0.256	0.350	0.899	0.983	0.249	0.453
% Clay (USDA)	0.282	0.816	0.840	0.638	0.886	0.004	0.042	0.220	0.123	0.117	0.056	0.125	0.116	0.092
Porosity	0.064	0.224	0.743	0.588	0.614	0.005	0.077	0.596	0.559	0.019	0.051	0.144	0.011	0.022
Ks [mm/d]	0.065	0.352	0.936	0.535	0.640	0.002	0.027	0.870	0.431	0.014	0.022	0.065	0.011	0.014

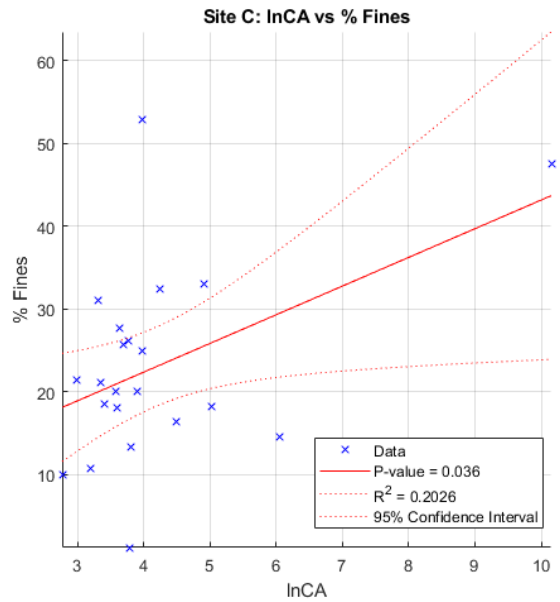

Fig 6.1. *Contributing Area Regression Curve*

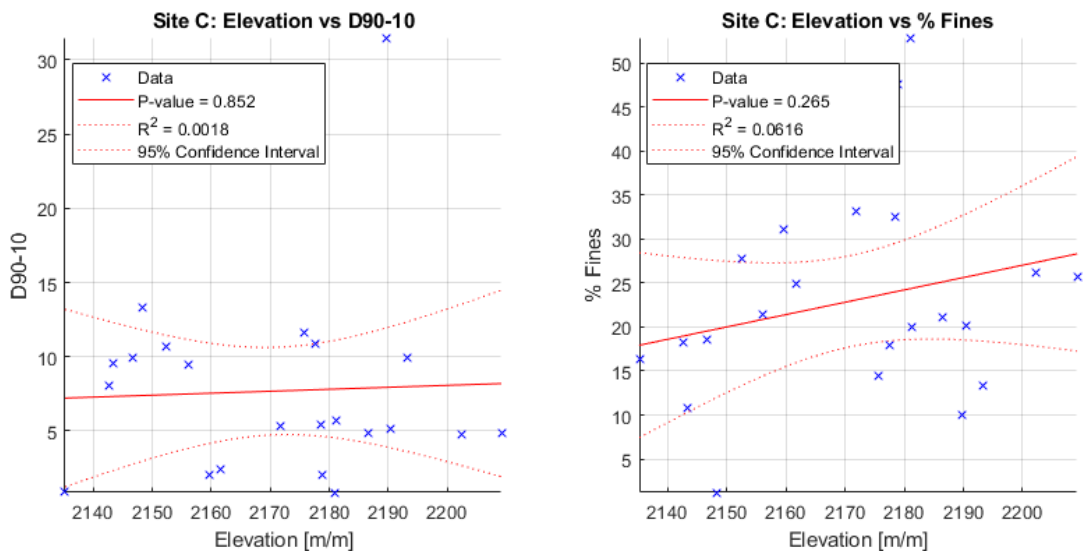

Fig 6.2. *Slope Regression Curves*

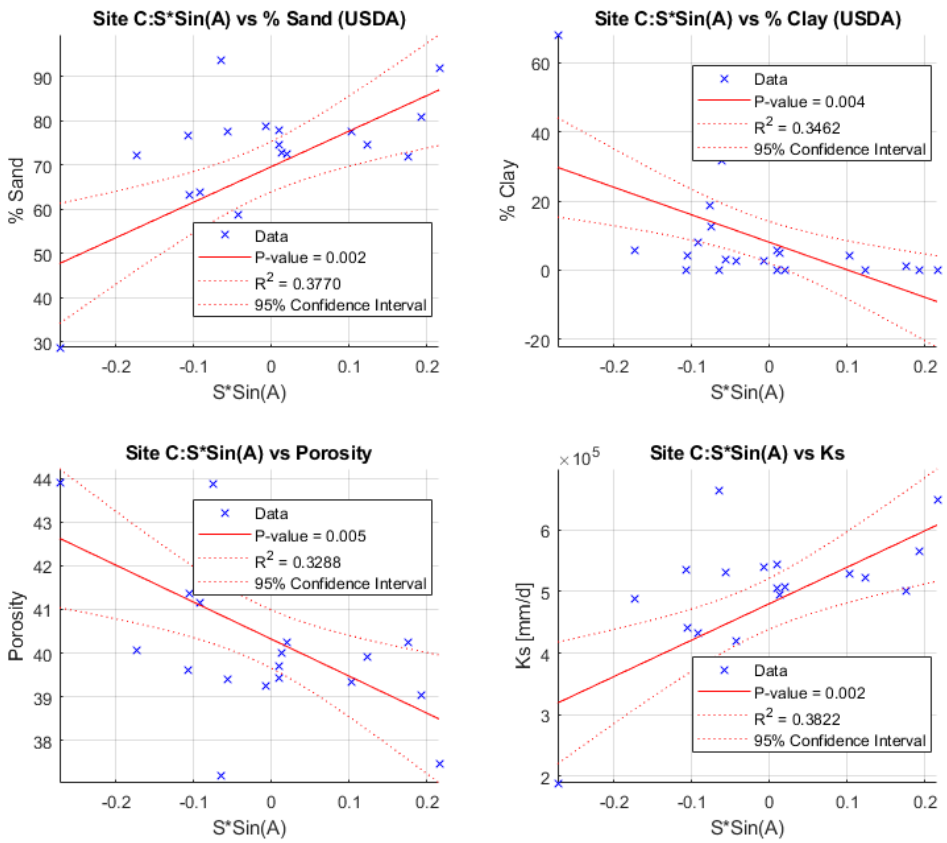

Fig. 6.3. *Eastness Regression Curves*

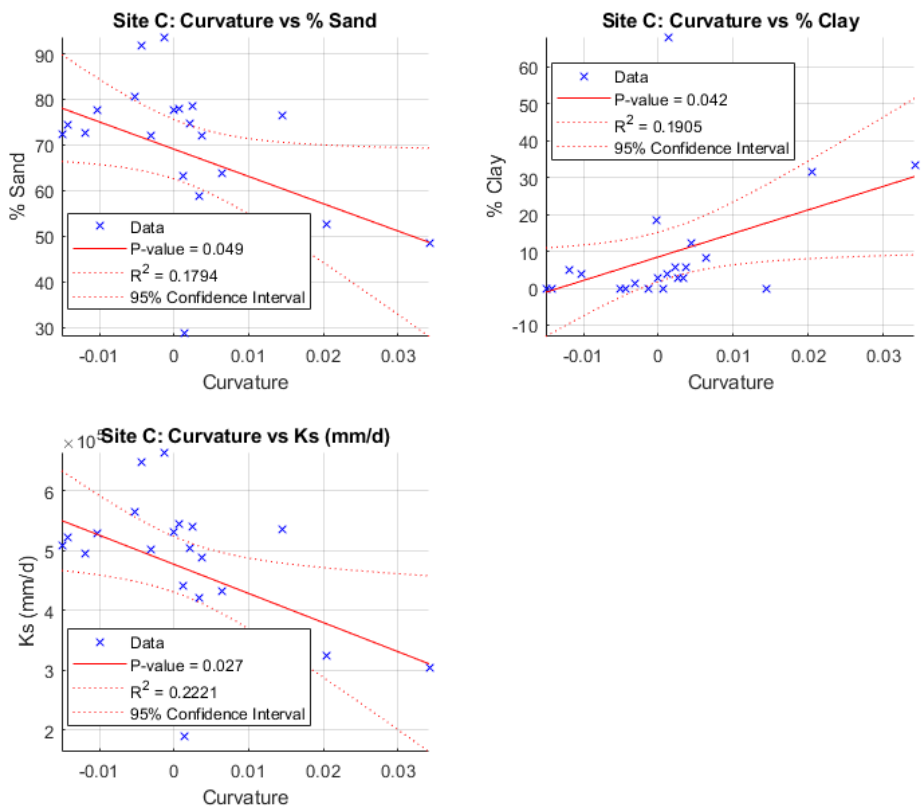

Fig. 6.4. *Curvature Regression Curves*

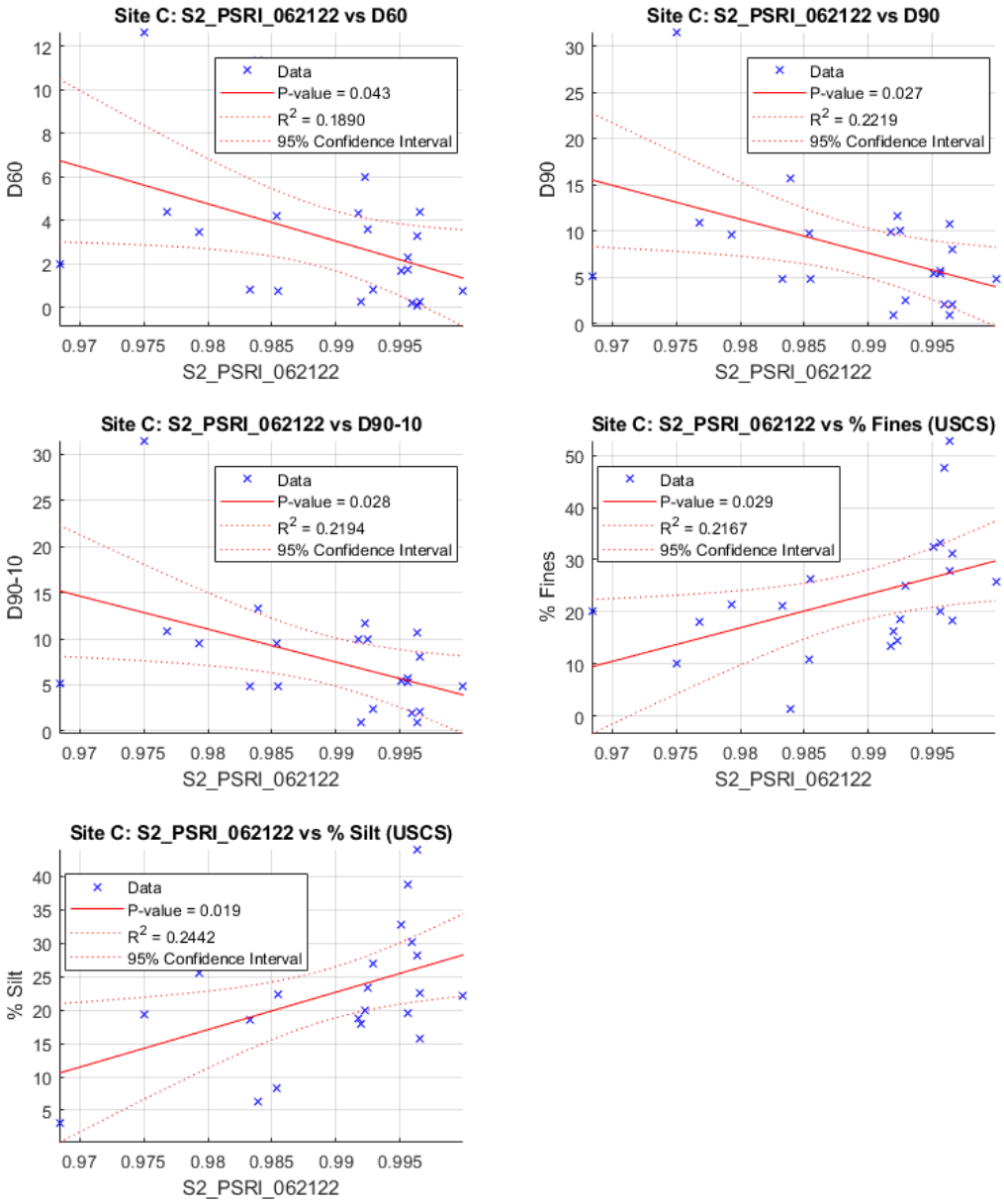

Fig. 6.5. *S2 PSRI Summer Solstice Regression Curves*

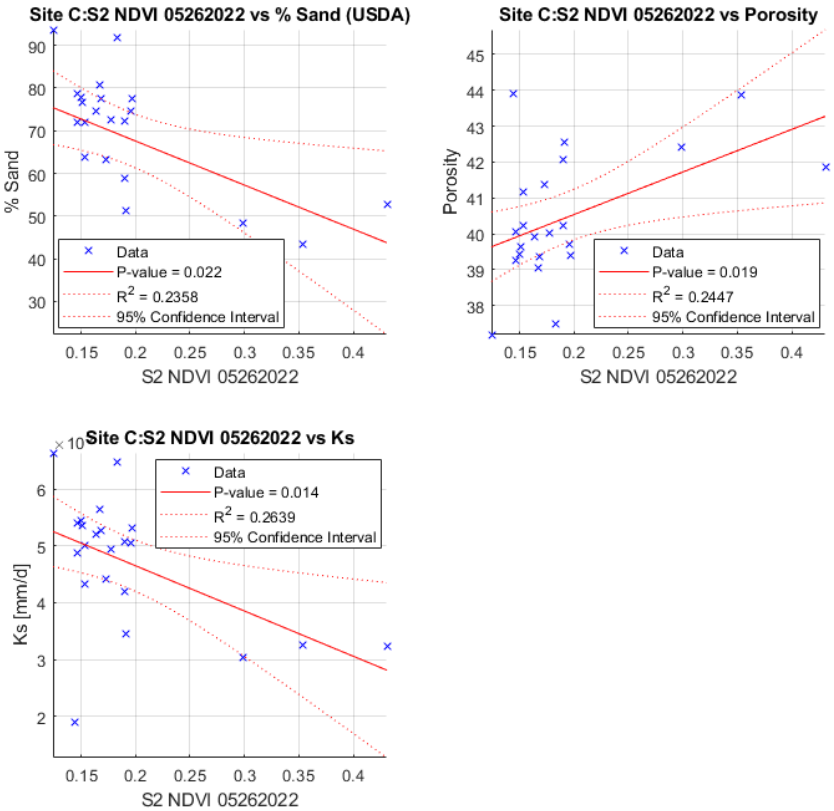

Fig. 6.6. *S2 NDVI 05/26/2022 Regression Curves*

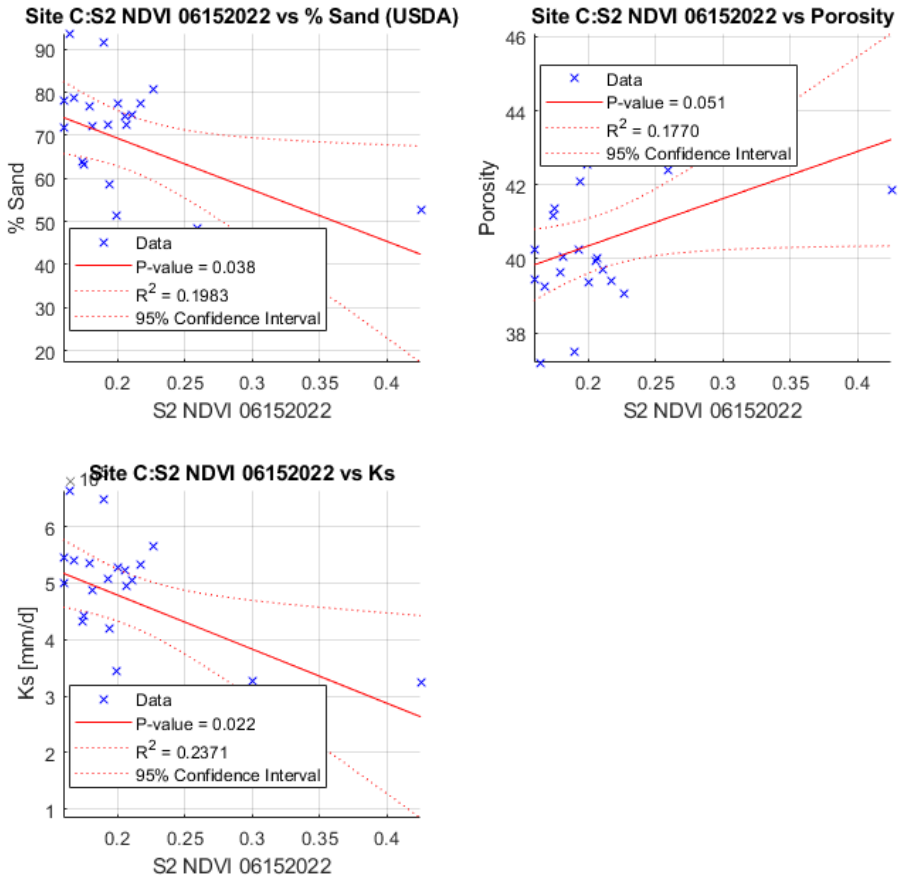

Fig. 6.7. *S2 NDVI 06/15/2022 Regression Curves*

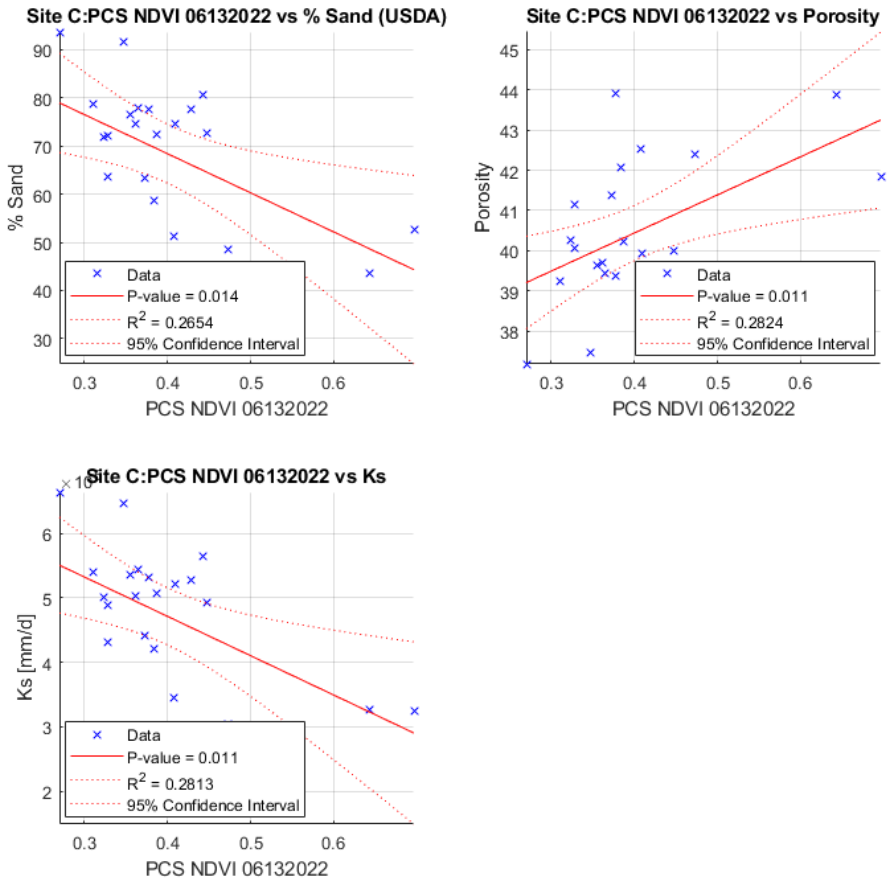

Fig. 6.8. *PCS NDVI 06/13/2022 Regression Curves*

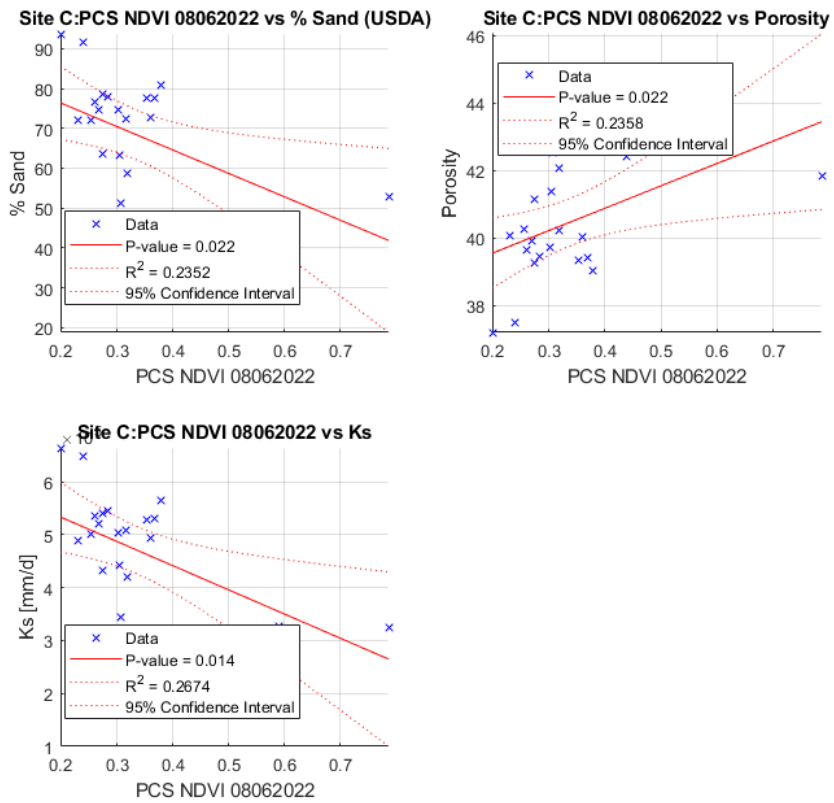

Fig. 6.9. *PCS NDVI 08/06/2022 Regression Curves*

Region D

Tables (2.10) and (2.11) display the strength and significance respectively of the relationships on Region D, host of the largest elevation difference between its highest and lowest sites and where much of the region was protected from the wind prevalent on other regions. Slope (Fig. 7.1) had a strong positive relationship with particle diameter percentiles and a strong negative relationship with percent fines. This is consistent with expectations and other regions as fines are generally not well retained as they are much more prone to movement. Northness (Fig. 7.2) is moderately negatively correlated with percent sand (USCS) and percent clay. The graph confidence intervals indicate these relationships could be positive or negative. These results cannot be used in a determination of positive or negative relationships. The expected behavior for a site with more sun exposure is fewer large particles and more small particles. Eastness (Fig. 7.3) had a strong negative relationship with particle diameter percentiles and percent gravel, and a moderate positive relationship with percent sand (USCS) and percent fines, which is within expectations as the more protected from wind the site is, the more likely smaller

particles will blow into the site and not be blown away. Summer sun exposure (Fig 7.4) had a strong negative correlation with particle diameter percentiles and percent gravel. This is expected as seen in other regions as direct sun exposure degrades soils. The *p-values* for percent sand (USCS) and percent fines are close but not significant, and they have correspondingly moderately positive relationships. Those two relationships can't be considered for this region because of their *p-values*, but they are further indicators of expected behavior for a site with more summer sun exposure. Winter sun exposure (Fig. 7.5) had a strongly positive relationship with particle diameter percentile and percent gravel. While particle sizes are more likely to be influenced by factors such as parent material, climate, and soil-forming processes, temperature changes may result in changes in heavy rain or snowmelt transporting fine particles away from those areas exposed to the winter sun. Snowmelt is more likely in this area due to small annual amounts of rainfall. Vegetation (Figs. 7.6, 7.7, 7.8, 7.9, 7.10) had a moderately to strongly positive relationship with percent clay like in other regions, further indicating vegetation type be considered further, specifically, grasses may better retain smaller particles.

Table 2.10. *Region D Linear Regression strength of correlation (r) values*

Site D: r	ln(CA)	Slope	Elevation	ln(aspect)	S*Cos(A)	S*Sin(A)	Curvature	S2 PSRI SS	S2 PSRI WS	S2 NDVI 05262022	S2 NDVI 06152022	LS NDVI 06142022	PCS NDVI 06132022	PCS NDVI 08062022
D10	0.022	0.786	0.032	0.137	0.123	-0.756	0.214	-0.908	0.691	-0.314	-0.205	-0.101	-0.247	-0.099
D30	0.081	0.781	0.026	0.223	-0.014	-0.674	0.137	-0.835	0.618	-0.330	-0.137	-0.042	-0.188	-0.067
D50	0.181	0.699	0.072	0.222	0.064	-0.713	0.069	-0.742	0.595	-0.300	-0.090	0.028	-0.191	-0.068
D60	0.199	0.672	0.105	0.265	0.049	-0.700	0.062	-0.688	0.569	-0.250	-0.028	0.102	-0.169	-0.063
D90	0.199	0.672	0.105	0.265	0.049	-0.700	0.062	-0.688	0.569	-0.250	-0.028	0.102	-0.169	-0.063
D90-10	-0.117	0.627	0.247	0.143	0.338	-0.631	-0.164	-0.615	0.628	-0.147	0.003	0.248	-0.131	-0.183
% Gravel (USCS)	0.005	0.700	0.136	0.351	0.182	-0.651	0.011	-0.715	0.615	-0.354	-0.149	0.015	-0.303	-0.220
% Sand (USCS)	0.050	-0.271	-0.234	-0.142	-0.475	0.477	0.193	0.407	-0.395	0.426	0.478	0.191	0.500	0.501
% Fines (USCS)	-0.227	-0.494	0.163	-0.273	0.079	0.485	-0.127	0.437	-0.377	0.124	-0.179	-0.168	-0.021	-0.190
% Sand (USDA)	0.356	0.132	-0.338	0.008	0.150	-0.388	0.028	-0.159	0.112	-0.131	0.027	-0.027	-0.042	0.149
% Silt (USDA)	-0.312	-0.268	0.308	-0.024	0.015	0.403	-0.059	0.220	-0.214	-0.057	-0.252	-0.275	-0.194	-0.321
% Clay (USDA)	-0.183	0.344	0.145	0.043	-0.478	0.028	0.081	-0.135	0.254	0.538	0.606	0.824	0.649	0.440
Porosity	-0.349	-0.167	0.334	-0.012	-0.111	0.396	-0.036	0.176	-0.139	0.085	-0.084	-0.049	-0.017	-0.194
Ks [mm/d]	0.377	0.092	-0.284	0.023	0.222	-0.362	0.046	-0.152	0.105	-0.212	-0.068	-0.181	-0.161	0.063

Table 2.11. *Region D Regression significance (p) values*

Site D: p-values	ln(CA)	Slope	Elevation	ln(aspect)	S*Cos(A)	S*Sin(A)	Curvature	S2 PSRI SS	S2 PSRI WS	S2 NDVI 05262022	S2 NDVI 06152022	LS NDVI 06142022	PCS NDVI 06132022	PCS NDVI 08062022
D10	0.931	0.000	0.900	0.588	0.626	0.000	0.395	0.000	0.001	0.205	0.416	0.690	0.324	0.697
D30	0.751	0.000	0.918	0.374	0.957	0.002	0.587	0.000	0.006	0.182	0.587	0.868	0.455	0.792
D50	0.472	0.001	0.777	0.377	0.801	0.001	0.785	0.000	0.009	0.227	0.722	0.911	0.448	0.788
D60	0.428	0.002	0.679	0.288	0.848	0.001	0.806	0.002	0.014	0.317	0.911	0.688	0.502	0.804
D90	0.428	0.002	0.679	0.288	0.848	0.001	0.806	0.002	0.014	0.317	0.911	0.688	0.502	0.804
D90-10	0.645	0.005	0.322	0.572	0.170	0.005	0.515	0.007	0.005	0.560	0.990	0.321	0.604	0.468
% Gravel (USCS)	0.984	0.001	0.590	0.153	0.469	0.003	0.966	0.001	0.007	0.149	0.556	0.953	0.221	0.380
% Sand (USCS)	0.844	0.276	0.350	0.575	0.046	0.046	0.442	0.093	0.105	0.078	0.045	0.447	0.035	0.034
% Fines (USCS)	0.364	0.037	0.519	0.273	0.757	0.041	0.615	0.070	0.123	0.625	0.477	0.506	0.934	0.450
% Sand (USDA)	0.147	0.603	0.170	0.976	0.551	0.112	0.913	0.530	0.657	0.603	0.916	0.916	0.869	0.556
% Silt (USDA)	0.208	0.283	0.214	0.924	0.952	0.097	0.816	0.381	0.393	0.822	0.314	0.269	0.440	0.195
% Clay (USDA)	0.467	0.163	0.565	0.867	0.045	0.911	0.749	0.593	0.309	0.021	0.008	0.000	0.004	0.068
Porosity	0.155	0.507	0.175	0.962	0.662	0.104	0.887	0.486	0.582	0.736	0.742	0.847	0.946	0.442
Ks [mm/d]	0.123	0.717	0.254	0.928	0.375	0.140	0.857	0.547	0.679	0.398	0.788	0.472	0.524	0.802

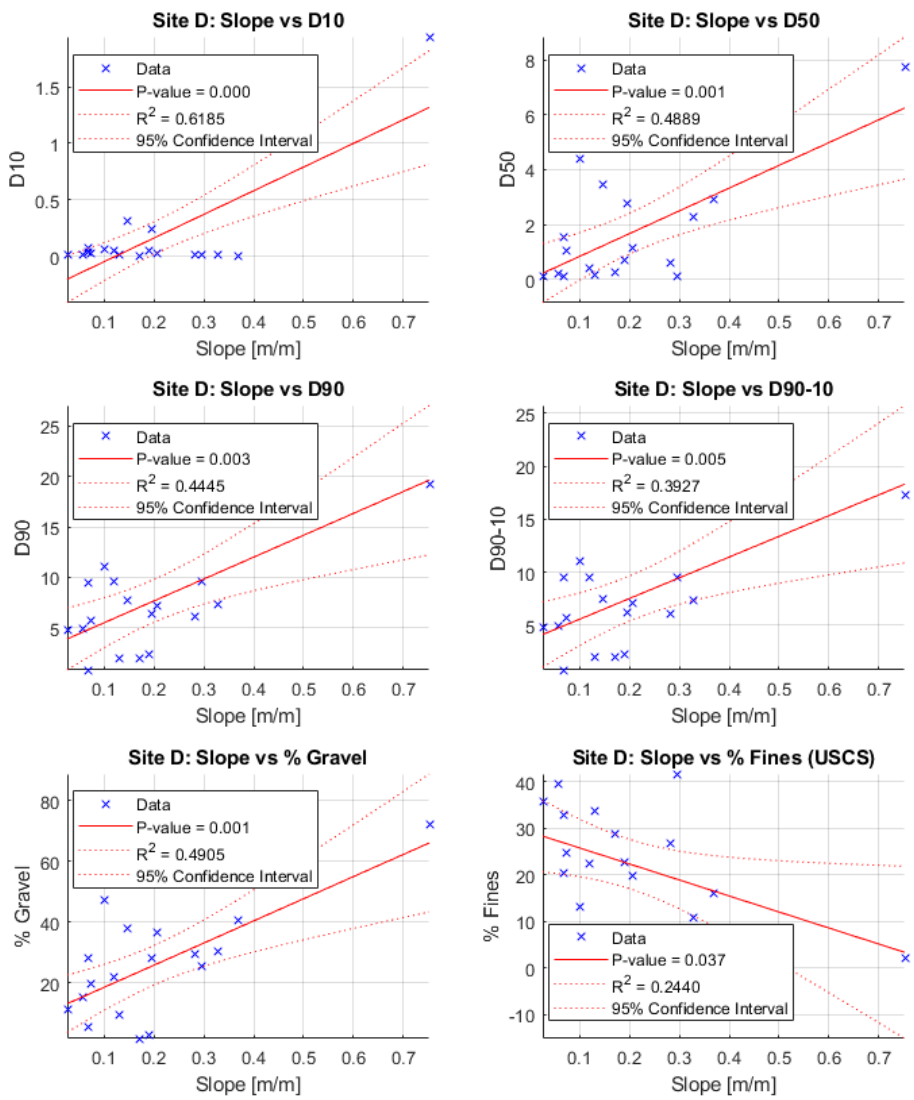

Fig. 7.1. *Slope Regression Curves*

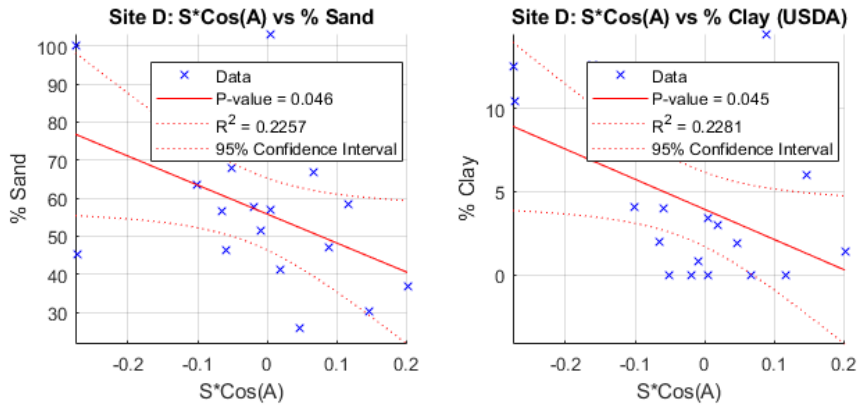

Fig. 7.2. *Northness Regression Curves*

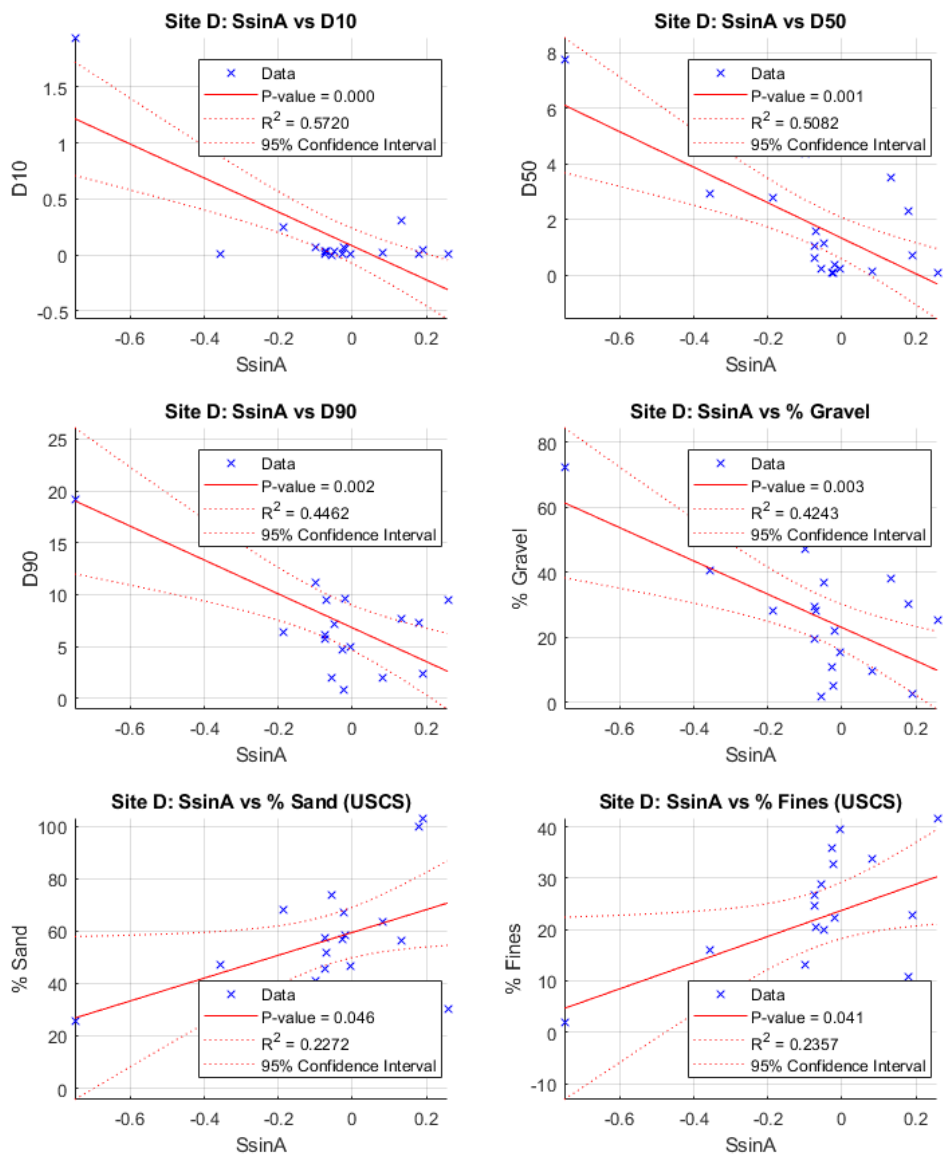

Fig. 7.3. *Eastness Regression Curves*

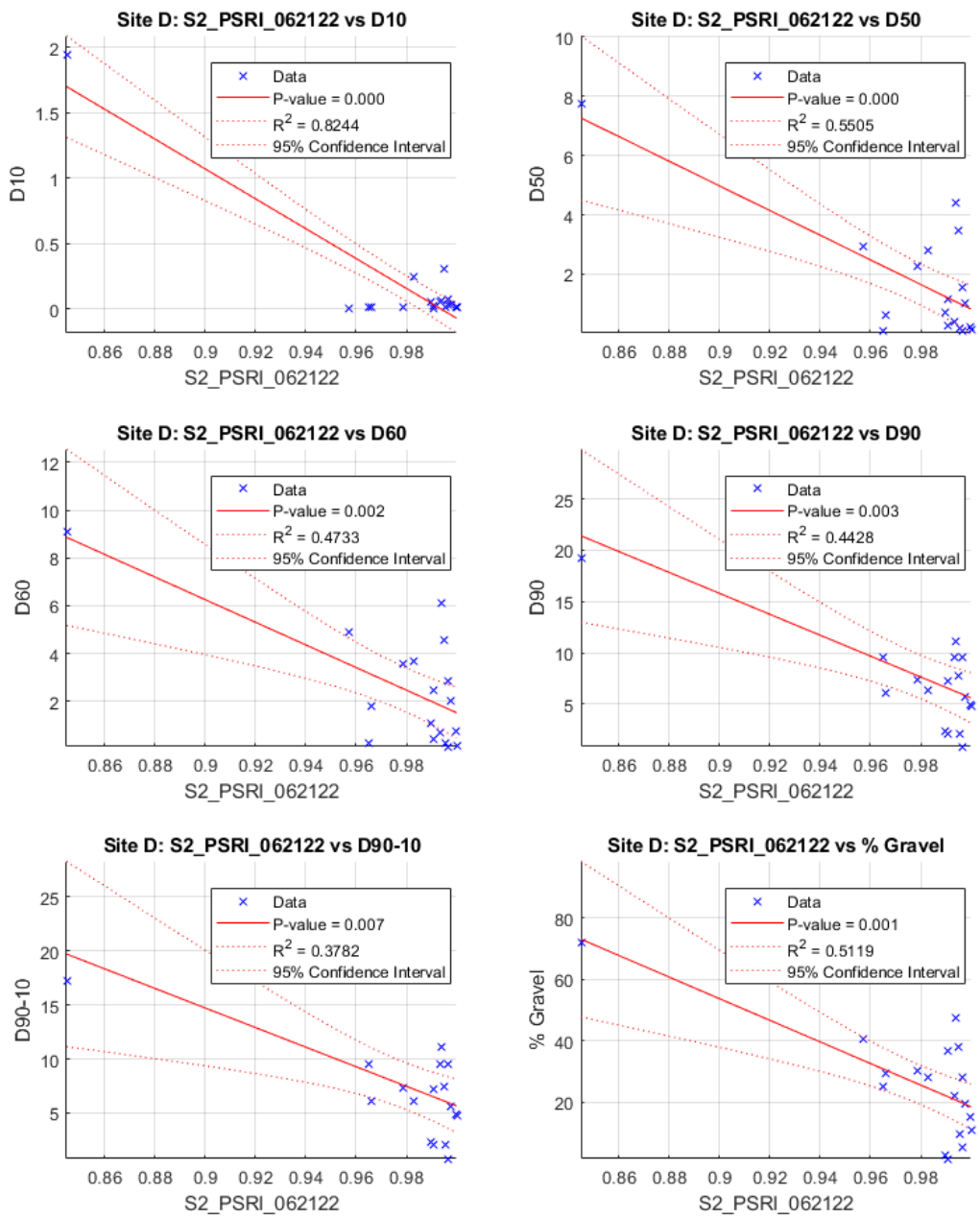

Fig. 7.4. *S2 PSRI Summer Solstice (06/21/2022) Regression Curves*

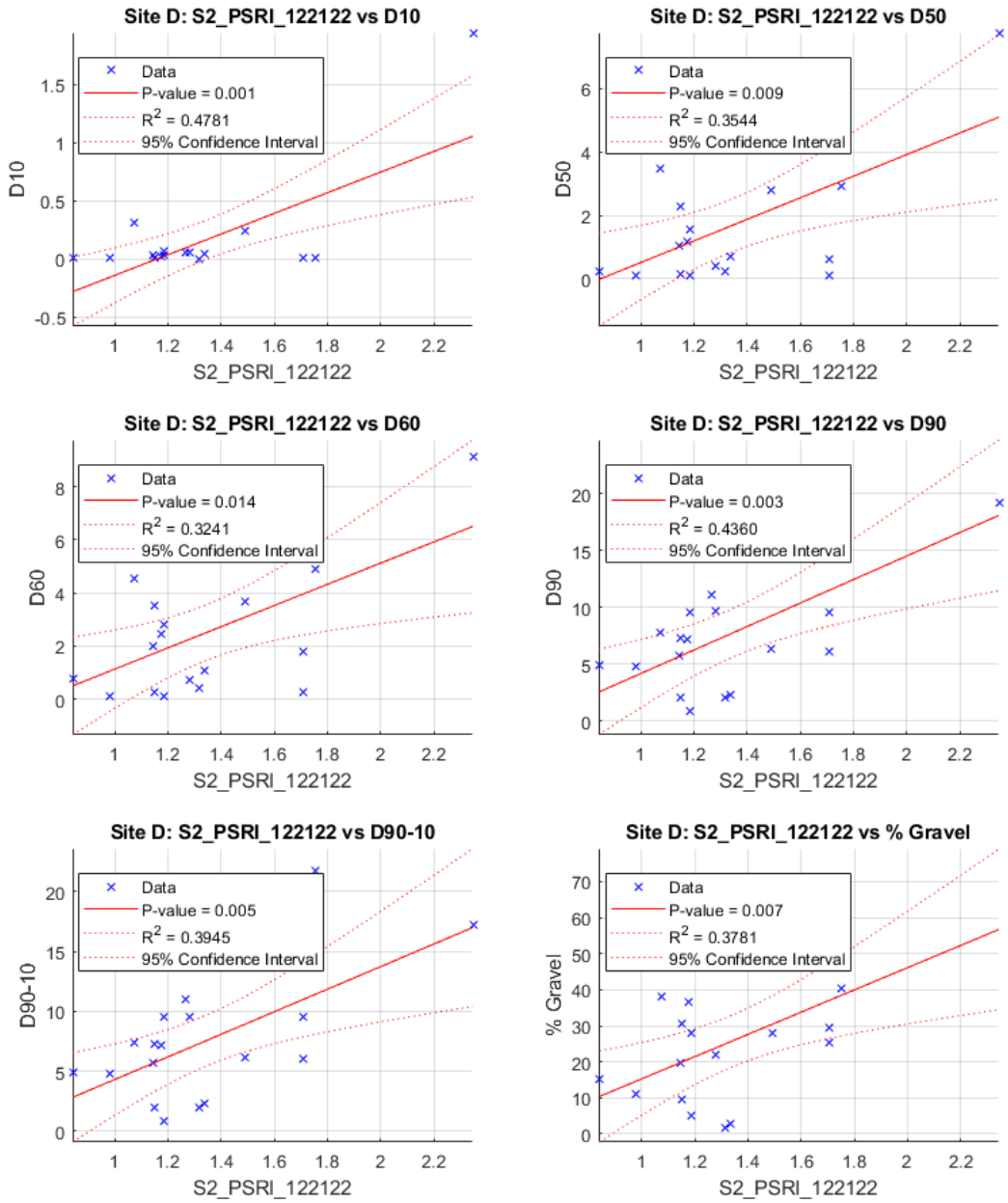

Fig. 7.5. *S2 PSRI Winter Solstice (12/21/2022) Regression Curves*

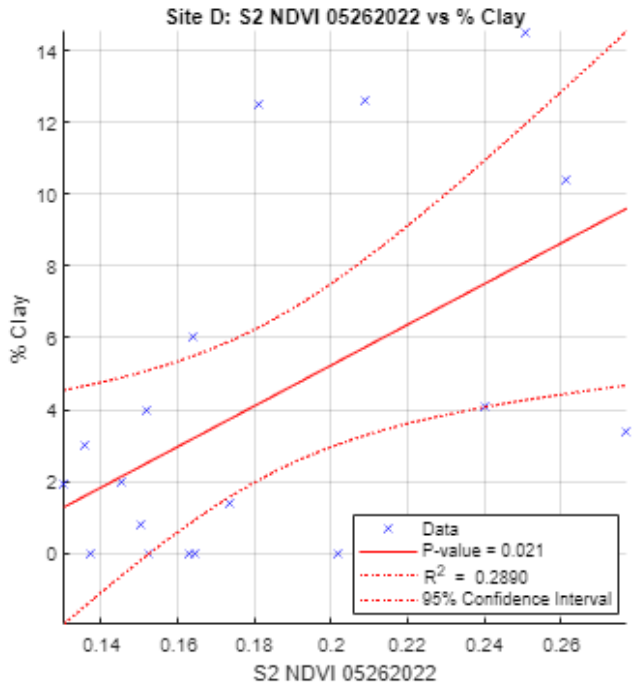

Fig. 7.6. *S2 NDVI 05/26/2022 Regression Curves*

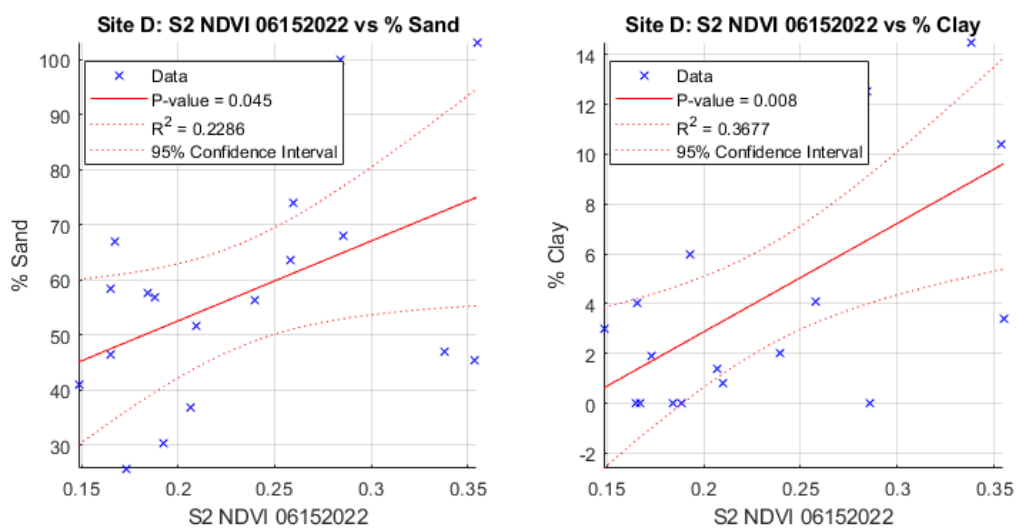

Fig. 7.7. *S2 NDVI 06/15/2022 Regression Curves*

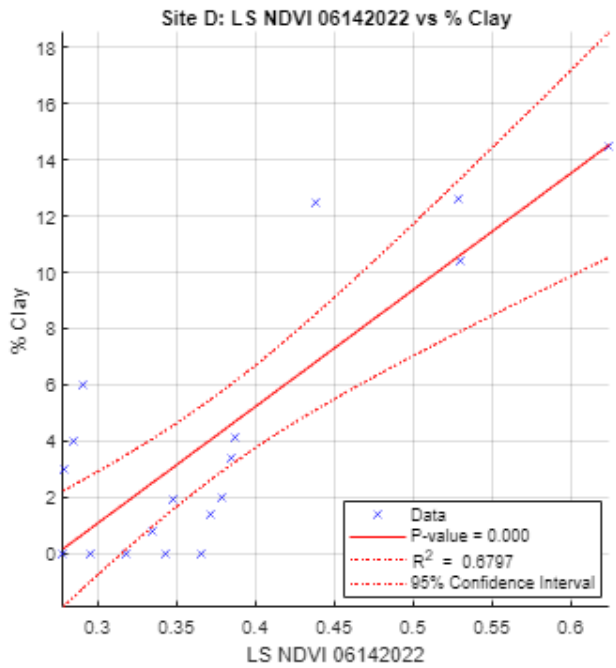

Fig. 7.8. *LS NDVI 06/14/2022 Regression Curves*

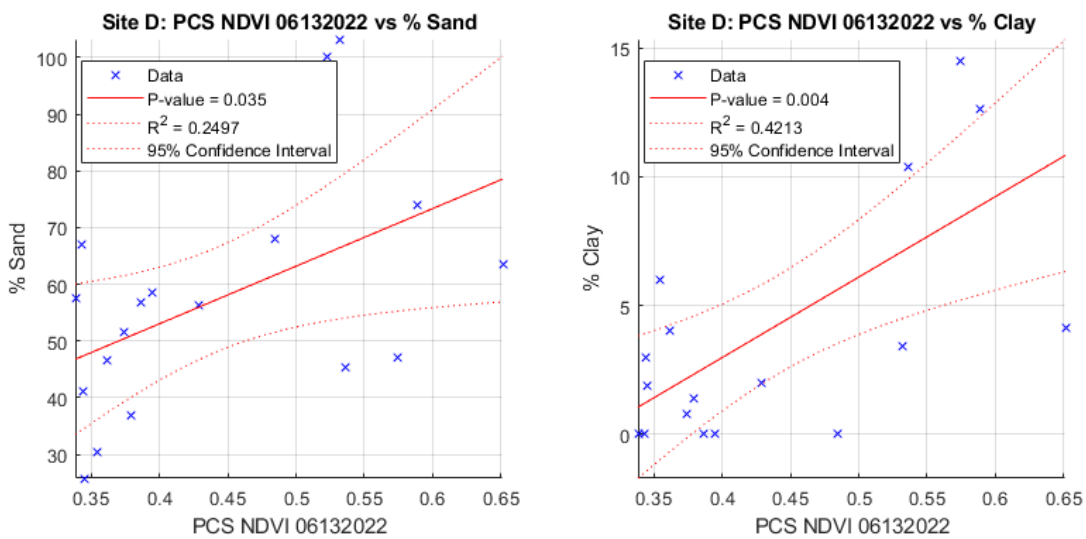

Fig. 7.9. *PCS NDVI 06/13/2022 Regression Curves*

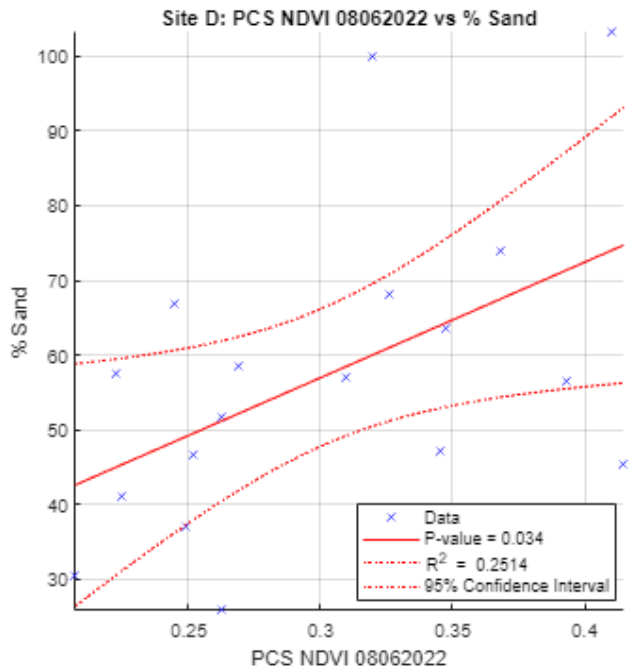

Fig. 7.10. *PCS NDVI 08/06/2022 Regression Curves*

Multiple Linear Regressions

Table (2.12) and Table (2.13) give the r^2 and p-values respectively for each region. All regions had extremely high correlations, but the ranch-wide collective had pointedly lower correlations. In general, p-values are influenced by several factors, including sample size, strength of correlation, and the level of significance. If a sample size is large enough, even a weak correlation can produce a significant p-value. This appears to be what is occurring with the ranch-wide analysis. Per Table (2.13), Region A's MLR had a strong correlation with porosity, Region B's MLR had a strong correlation with all particle diameter percentiles, Region C's MLR had a strong correlation with percent fines, and Region D's MLR had a strong correlation with D10 and percent clay. Ranch-wide analysis resulted in weak correlation with all particle diameter percentiles and USCS classifications (percent gravel, percent sand, and percent fines), percent clay, and hydraulic conductivity. There is a clear disconnect between variable predictabilities across the ranch. It is likely these are driven by unique texture trends across each region.

Ranch-wide and regional analysis gave an estimate of coefficients and intercepts for MLR equations that best fit the data of their respective regions (Tables 2.14, 2.15, 2.16, 2.17). The "ones" column indicates the intercept. This is the value that, if considerably large compared to the coefficients, indicates that either there are variables not considered in the MLR that drive the base value of the

intercept, or that there are no variables that can predict the base value of the intercept. Coefficients close to zero have little to no impact on the respective dependent variable.

Ranch-wide MLR analysis resulted in most variables being correlated (Table 2.14). A point of interest is that ranch-wide r^2 were significantly lower than regional r^2. As the coefficient of determination is a measure of variance accountability, the most likely explanation is each site has unique data and corresponding trends that, once combined, increase variance and decrease the ability of an MLR equation to capture that variance. Regional MLR analysis will show these unique trends and what variables are considered important to different regions. A noteworthy point is that five separate vegetation dates were included in MLR and, while the data for each date is unique, it is possible for vegetation's importance to be overestimated.

Table 2.12. *MLR Coefficients of Determination (r^2)*

r^2	Region A	Region B	Region C	Region D	Ranch-wide
D10	0.63	0.94	0.49	0.99	0.33
D30	0.81	0.94	0.55	0.95	0.35
D50	0.79	0.93	0.74	0.89	0.37
D60	0.79	0.92	0.77	0.87	0.37
D90	0.80	0.88	0.76	0.97	0.38
D90-10	0.80	0.88	0.75	0.96	0.37
Gravel(USCS)	0.83	0.87	0.80	0.87	0.38
Sand(USCS)	0.80	0.86	0.61	0.72	0.33
Fines(USCS)	0.86	0.73	0.95	0.95	0.33
Sand(USDA)	0.92	0.44	0.83	0.82	0.22
Silt(USDA)	0.92	0.56	0.67	0.76	0.14
Clay(USDA)	0.85	0.54	0.78	0.99	0.27
porosity	0.93	0.46	0.82	0.80	0.19
Ks_mmday	0.88	0.45	0.80	0.87	0.28

Table 2.13. *MLR p-values*

p-values	Region A	Region B	Region C	Region D	Ranch-wide
D10	0.79	0.01	0.89	0.02	0.00
D30	0.34	0.01	0.79	0.15	0.00
D50	0.40	0.01	0.32	0.37	0.00
D60	0.41	0.01	0.25	0.42	0.00
D90	0.37	0.05	0.27	0.07	0.00
D90-10	0.37	0.05	0.30	0.09	0.00
Gravel(USCS)	0.29	0.06	0.19	0.42	0.00
Sand(USCS)	0.37	0.07	0.67	0.81	0.01
Fines(USCS)	0.21	0.37	0.00	0.13	0.00
Sand(USDA)	0.07	0.93	0.12	0.59	0.16
Silt(USDA)	0.06	0.78	0.53	0.74	0.65
Clay(USDA)	0.23	0.80	0.24	0.02	0.04
porosity	0.05	0.91	0.14	0.64	0.27
Ks_mmday	0.14	0.92	0.18	0.43	0.03

Ranch-wide MLR analysis shows that most MLR equations were considered significant (Table 2.13), excluding only percent sand (USDA), percent silt, and porosity. These relationships, unlike regional relationships, had weak r^2 with a maximum across the variables of 0.38. Vegetation was the only consistently heavily weighted variable but its negatively was exceptionally date-dependent, fluctuating greatly for each variable (Table 2.14).

Outside of vegetation, several smaller coefficients were present for different textures. D10 weighed summer exposure positively and winter sun exposure negatively. D30 weighed winter sun exposure negatively. D90 and D90-10 weighed slope positively and curvature negatively. Percent sand (USCS) weighed natural log of contributing area, elevation, Northness, Eastness, and winter sun exposure negatively, and summer sun exposure positively. Percent fines weighed slope negatively. Percent clay weighed slope and Eastness negatively, and elevation positively. Hydraulic conductivity weighed elevation and curvature negatively. The intercepts were significantly larger than the variable coefficients for all but D10 and D30. This suggests that, according to the MLR equations, these variables are certainly having an effect, but they are not driving the base value and may not be sufficient as the only inputs in a model. This is expected when combining highly variable regions with unique data and trends.

Table 2.14. *Ranch-wide Standardized Coefficients and Intercepts*

Ranch-wide	Ones	ln(CA)	Slope	Elevation	Aspect	S*Cos(A)	S*Sin(A)	Curvature	S2 PSRI SS	S2 PSRI WS	S2 NDVI 05262022	S2 NDVI 06152022	LS NDVI 06142022	PCS NDVI 06132022	PCS NDVI 08062022
D10	0.74	0.43	-0.37	-0.42	0.03	0.52	-0.09	-0.26	0.91	-1.55	-0.85	1.62	-0.46	-1.97	1.72
D30	1.32	0.12	0.24	-0.44	-0.63	0.54	0.55	-0.30	0.21	-1.33	-0.65	1.63	-0.18	-2.33	1.25
D50	1.83	-0.02	0.53	-0.32	-0.69	0.33	0.39	-0.61	0.36	-0.78	-1.05	0.88	0.05	-2.34	1.44
D60	2.05	-0.08	0.60	-0.26	-0.68	0.24	0.31	-0.67	0.37	-0.53	-1.34	0.56	0.14	-2.16	1.45
D90	2.89	-0.35	0.64	-0.16	-0.48	0.26	-0.08	-0.58	0.10	-0.32	-1.62	-0.66	0.50	-1.08	0.94
D90-10	2.91	-0.38	0.67	-0.14	-0.49	0.24	-0.07	-0.58	0.06	-0.26	-1.61	-0.75	0.53	-1.01	0.88
Gravel(USCS)	2.73	-0.12	0.15	-0.29	-0.39	0.09	0.08	-0.55	0.31	-0.70	-1.18	0.19	0.38	-1.86	1.16
Sand(USCS)	3.52	-0.44	0.15	-0.43	-0.30	-0.62	-0.42	-0.21	-0.53	0.44	-0.15	0.34	-0.79	-0.08	-0.48
Fines(USCS)	2.83	-0.02	-0.96	-0.01	0.03	-0.05	-0.25	0.18	-0.43	-0.45	0.64	-1.06	-0.31	1.34	-1.47
Clay(USDA)	3.10	-0.27	-0.90	0.47	-0.26	-0.41	-0.79	-0.33	0.04	-0.56	1.11	-0.86	0.68	-0.68	-0.35
Ks_mmday	3.58	-0.19	-0.01	-0.49	-0.28	-0.25	-0.22	-0.41	-0.17	-0.12	-0.93	0.23	-0.50	-0.52	0.27

Region A showed only one significant MLR correlation (Table 2.13). The intercepts and coefficients for porosity are given in Table (2.15) and indicate that all the coefficients are small compared to the intercept. With all coefficients being below ~15% of the intercept, this MLR suggests no variables in the current selection have great effect on the baseline value. However, of these coefficients, the most impactful ones were the natural log of contributing area, slope, Northness, summer sun exposure, and 08/06/22 vegetation and were all negative. These variables ultimately result in the excellent r^2 of 0.93 (Table 2.12).

Table 2.15. *Region A Standardized Coefficients and Intercepts*

Region A	Ones	ln(CA)	Slope	Elevation	Aspect	S*Cos(A)	S*Sin(A)	Curvature	S2 PSRI SS	S2 PSRI WS	S2 NDVI 05262022	S2 NDVI 06152022	LS NDVI 06142022	PCS NDVI 06132022	PCS NDVI 08062022
porosity	3.71	-0.33	-0.38	-0.20	-0.28	-0.35	-0.24	-0.11	-0.35	-0.30	0.09	-0.25	-0.19	-0.30	-0.54

Region B displayed several significant MLR correlations (Table 2.13), specifically with particle diameter percentiles. The intercepts and coefficients (Table 2.16) indicate that natural log of contributing area, curvature, Eastness, and winter sun exposure were consistently weighted heavily across all percentiles. The coefficients for natural log of contributing area were negative for all percentiles but D10. Curvature's coefficients were positive except for D10. Eastness' were all positive and winter sun exposure coefficients were all negative. The intercepts also increased in importance as particle diameter percentile increased.

Individual percentiles had additional variables weighed heavily for their respective MLRs. D10's unique coefficients were a positive slope and a vegetation whose strength and negativity were highly date dependent. D30's, D50's, and D60's additional coefficients were negative aspects. D90's and D90-10's were vegetation. MLR analysis across this region gave predictably inconsistent vegetation coefficients. The MLR of these inputs with diameter percentiles resulted in strong r^2 across all percentiles, with all being above 0.9 except for D90 and D90-10 at 0.88.

Table 2.16. *Region B Standardized Coefficients and Intercepts*

Region B	Ones	ln(CA)	Slope	Elevation	Aspect	S*Cos(A)	S*Sin(A)	Curvature	S2 PSRI SS	S2 PSRI WS	S2 NDVI 05262022	S2 NDVI 06152022	LS NDVI 06142022	PCS NDVI 06132022	PCS NDVI 08062022
D10	1.02	1.46	-1.00	0.23	-0.02	-0.34	0.96	-1.14	-0.01	-1.35	-1.06	-0.39	0.54	-0.93	2.04
D30	1.15	-1.35	-0.26	-0.29	-1.15	0.09	1.14	1.68	0.42	-1.95	-0.62	1.37	-0.03	-0.09	-0.11
D50	1.70	-1.30	-0.38	-0.41	-1.08	0.00	1.17	1.57	0.53	-2.03	-0.57	0.60	-0.01	0.12	0.08
D60	1.97	-1.22	-0.47	-0.43	-0.92	0.04	1.06	1.39	0.68	-2.06	-0.63	0.31	-0.19	0.22	0.25
D90	2.60	-1.35	0.21	-0.39	-0.03	0.24	0.57	1.11	0.28	-1.15	-0.34	-1.12	-0.98	0.82	-0.47
D90-10	2.58	-1.37	0.22	-0.39	-0.03	0.25	0.55	1.12	0.28	-1.13	-0.32	-1.12	-0.98	0.84	-0.49

Region C's MLR equations, much like Region A, only produced one significant relationship (Table 2.13) in percent fines. There were few heavily weighted variables, with slope, Eastness, curvature, winter sun exposure, and vegetation being the most impactful (Table 2.17). Only vegetation was above 40% of the intercept, but all were above 30%. Slope and winter sun exposure had positive coefficients while Eastness and curvature had negative. Vegetation fluctuated from highly negative to highly positive depending on the date. It is noteworthy that while these results run counter to expectation and previous linear regression analysis, MLR still considers those variables to be important and produced a strong r^2 of 0.95 (Table 2.12).

Table 2.17. *Region C Standardized Coefficients and Intercepts*

Region C	Ones	ln(CA)	Slope	Elevation	Aspect	S*Cos(A)	S*Sin(A)	Curvature	S2 PSRI SS	S2 PSRI WS	S2 NDVI 05262022	S2 NDVI 06152022	LS NDVI 06142022	PCS NDVI 06132022	PCS NDVI 08062022
Fines(USCS)	1.91	0.08	0.72	-0.27	-0.47	-0.45	-0.79	-0.66	-0.10	0.83	0.08	-2.13	-1.11	1.29	1.06

Region D's MLR equations displayed two significant relationships in D10 and percent clay (Table 2.13). The coefficients in Table (2.18) show that several variables have substantial impact on D10, but not percent clay. Slope, Eastness, curvature, winter sun exposure, and vegetation were weighed heavily in D10. Slope, elevation, curvature, summer sun exposure, winter sun exposure, and vegetation were heavily weighted coefficients for percent clay. Slope's coefficient was positive for D10 while Eastness, curvature, and winter sun exposure were negative. Slope, summer sun exposure, and winter sun exposure's coefficients were negative for percent clay, and elevation and curvature's coefficients were positive. Slope and winter sun exposure had the highest impact on D10, and vegetation had the highest impact on percent clay. Vegetation's weight, like in all other regions, fluctuated negativity depending on the date.

Table 2.18. *Region D Standardized Coefficients and Intercepts*

Region D	Ones	ln(CA)	Slope	Elevation	Aspect	S*Cos(A)	S*Sin(A)	Curvature	S2 PSRI SS	S2 PSRI WS	S2 NDVI 05262022	S2 NDVI 06152022	LS NDVI 06142022	PCS NDVI 06132022	PCS NDVI 08062022
D10	0.97	0.34	1.31	-0.25	0.18	-0.25	-0.49	-0.72	0.03	-1.25	1.50	-0.90	-1.23	-1.20	1.94
Clay(USDA)	0.77	-0.32	-0.35	0.47	-0.35	0.07	0.26	0.85	-0.62	-0.43	-2.26	0.06	1.51	1.76	-1.41

Conclusion

Laboratory analysis was conducted on 86 soil samples from 86 sample sites from four regions throughout this report to determine soil textures, USCS and USDA classifications, and pedotransfer function outputs porosity and hydraulic conductivity. Satellite-obtained topography and vegetation data were compiled and both linear and multiple linear regression analyses were performed to assess the potential relationships between these variables. Highly variable topography has historically caused large errors in soil characteristic prediction, and this report investigated potential quantifiable relationships across a highly variable region in Maxwell Ranch.

Several relationships between soil textures, topography, and vegetation were observed within this report. The natural log of contributing area was positively correlated with percent fines across most regions. Slope was positively correlated with percent gravel and negatively correlated with percent fines across half the regions. Summer sun exposure was negatively correlated with moderate to D60, D90, D90-10 and percent gravel in most regions. Eastness was positively correlated with all particle diameter percentiles and percent gravel across half the regions. Winter sun exposure was positively correlated with D10 and D30 across half the regions. Vegetation had the most interesting results, with much of its correlation appearing to depend on vegetation type. Unrelated to vegetation type, there was a negative correlation with sand (USDA) in half the regions. In regions with mostly grasses or shrubs, vegetation had a positive correlation with clay and a negative correlation with hydraulic conductivity. In regions with mostly tree cover, there was no correlation. Further study is needed on the effect of vegetation type on soil textures.

MLR analysis considered all input variables, weighing them against each other by creating an equation for each texture variable that would best predict and account for variance. These equation outputs confirmed that highly variable regions are difficult to predict and introduce considerable error. Within this report the regions appeared to have unique trends and data that, when combined in ranch-wide analysis, caused a significant drop in prediction strength and variance accountability. MLR analysis as a whole output equations whose coefficients' negativity would vary regionally. An outlier even in this was vegetation, which fluctuated heavily across different dates. Even with these fluctuations, slope,

curvature, Eastness, winter sun exposure, and vegetation were commonly the most heavily weighed across all regions.

REFERENCES

Amirian-Chakan, Alireza, et al. “Some Practical Aspects of Predicting Texture Data in Digital Soil Mapping.” Soil & tillage research 194 (2019): 104289–. Web.

Anand, Mallekedi, Anuj Jain, and Manoj Kumar Shukla. “An Optimized Deep Network Based Soil Texture Prediction and Vegetation Analysis Using Satellite Image Database.” Concurrency and Computation 35.7 (2023): n. page. Web.

ASTM Standard C117-17, 2017, “Standard Test Method for Materials Finer than 75-µm (No. 200) Sieve in Mineral Aggregates by Washing,” ASTM International, West Conshohocken, PA, 2017, DOI: 10.1520/C0117-17, www.astm.org.

ASTM Standard D2167-15, 2015, “Standard Test Method for Density and Unit Weight of Soil in Place by the Rubber Balloon Method,” ASTM International, West Conshohocken, PA, 2017, DOI: 10.1520/D2167-15, www.astm.org.

ASTM Standard D2216-19, 2019, “Standard Test Methods for Laboratory Determination of Water (Moisture) Content of Soil and Rock by Mass,” ASTM International, West Conshohocken, PA, 2019, DOI: 10.1520/D2216-19, www.astm.org.

ASTM Standard D422-63, 2007, “Standard Test Method for Particle-Size Analysis of Soils,” ASTM International, West Conshohocken, PA, 2007, DOI: 10.1520/D2167-15, www.astm.org.

ASTM Standard D4318-17e1, 2017, “Standard Test Methods for Liquid Limit, Plastic Limit, and Plasticity Index of Soils,” ASTM International, West Conshohocken, PA, 2018, DOI: 10.1520/D4318-17E01, www.astm.org.

ASTM Standard D6913/d6913m-17, 2017, “Standard Test Methods for Particle-Size Distribution (Gradation) of Soils Using Sieve Analysis,” ASTM International, West Conshohocken, PA, 2021, DOI: 10.1520/D6913_D6913M-17, www.astm.org.

ASTM Standard D7928-21e1, 2021, “Standard Test Method for Particle-Size Distribution (Gradation) of Fine-Grained Soils Using the Sedimentation (Hydrometer) Analysis,” ASTM International, West Conshohocken, PA, 2021, DOI: 10.1520/D7928-21E01, www.astm.org.

B. Hofmann-Wellenhof, H. Lichtenegger and J. Collins, 2001. “GPS - theory and practice.” Section 10.2.1. p. 282.

Bandara, R., J.P. Walker, C. Ruediger. 2014. “Towards soil property retrieval from space: Proof of concept using in situ observations.” J. Hydrology. 512: 27-38. doi: 10.1016/j.hydrol.2014.02.031.

Bradbury, Michael, et al., 2016. “Next-Generation NATO Reference Mobility Model (NG0NRMM).” Technical Report STO-AVT-ET-148, North Atlantic Treaty Organization (NATO) Science and Technology Organization (STO). Retrieved from https://apps.dtic.mil/sti/citations/AD1011267

Channarayappa, and D. P. Biradar. Soil Basics, “Management and Rhizosphere Engineering for Sustainable Agriculture.” Boca Raton, FL: CRC Press, 2019. Web.

Corps of Engineers, Humboldt Mfg. Co. 2013. Corps of Engineers Cone Penetrometer Product Manual H-4120H, H-4120HA. Retrieved from https://www.yumpu.com/en/document/view/11426674/corps-of-engineers-cone-penetrometer-humboldt-mfg-co

Cosby, B.J., G.M. Hornberger, R.B. Clapp, T.R. Ginn. 1984. “A statistical exploration of the relationships of soil-moisture characteristics to the physical properties of soils.” Water Resour. Res. 20: 682-690. Doi:10.1029/WR020i006p00682

David Eberly 1999. “Least Squares Fitting of Data” (Geometric Tools, LLC), pp. 3.

Dingman, S. L. “Physical Hydrology.” Third edition. Long Grove, Illinois: Waveland Press, Inc., 2015. Print.

Durner, W., Iden, S. C., and von Unold, G. (2017), “The integral suspension pressure method (ISP) for precise particle-size analysis by gravitational sedimentation.” Water Resour. Res., 53, 33– 48, doi:10.1002/2016WR019830.

E.J.Krakiwsky, and D.E.Wells, 1971. “Coordinate Systems In Geodesy.” (GEODESY AND GEOMATICS ENGINEERING, UNB), LECTURE NOTES, No16, 1971, pp. 18-38

Farr, John V., Meier, Roger W., Perkins, William E., 1992. “Strength Property Estimation for Dry, Cohesionless Soils Using the Military Cone Penetrometer.” Technical Report GL-92-5, U.S. Army Engineer Waterways Experiment Station, Vicksburg, MS. Retrieved from https://www.researchgate.net/publication/235091847_Strength_Property_Estimation_for_Dry_Cohesionless_Soils_Using_the_Military_Cone_Penetrometer.

Florinsky, Igor V. “Digital Terrain Analysis in Soil Science and Geology.” Second edition. London, UK: Academic Press is an imprint of Elsevier, 2016. Print.

Hengl, Tomislav, Gerard B.M. Heuvelink, and David G. Rossiter. “About Regression-Kriging: From Equations to Case Studies.” Computers & geosciences 33.10 (2007): 1301–1315. Web.

Khorram, Siamak. “Remote Sensing.” New York: Springer, 2012. Print.

Kim J-T, Im D-U, Choi H-J, Oh J-W, Park Y-J. 2021. “Development and Performance Evaluation of a Bevameter for Measuring Soil Strength. Sensors.” 2021; 21(4):1541. https://doi.org/10.3390/s21041541

Kopačková, V.; Ben-Dor, E.; Carmon, N.; Notesco, G. “Modelling Diverse Soil Attributes with Visible to Longwave Infrared Spectroscopy Using PLSR Employed by an Automatic Modelling Engine.” Remote Sens. 2017, 9, 134. https://doi.org/10.3390/rs9020134

Lancaster, P. and Šalkauskas, K. “Curve and Surface Fitting: An Introduction.” London: Academic Press, 1986.

Lee, Richard, (1964). “Potential Insolation As A Topoclimatic Characteristic Of Drainage Basins.” International Association of Scientific Hydrology. Bulletin, 9:1, 27-41, DOI: 10.1080/02626666409493652

Masek, J.G., Vermote, E.F., Saleous, N., Wolfe, R., Hall, F.G., Huemmrich, F., Gao, F., Kutler, J., and Lim, T.K. (2006). “A Landsat surface reflectance data set for North America.” 1990-100, IEEE Geoscience and Remote Sensing Letters. 3:68-72.

Marcin Ligas, and Piotr Banasik, 2011. “Conversion between Cartesian and geodetic coordinates on a rotational ellipsoid by solving a system of nonlinear equations (GEODESY AND CARTOGRAPHY).” Vol. 60, No 2, 2011, pp. 145-159

Mark, D. M., (1988), “Network models in geomorphology.” Chapter 4 in Modelling in Geomorphological Systems, Edited by M. G. Anderson, John Wiley., p.73-97.

METER Group AG. (2021). *PARIO – METER Group*. Retrieved from https://library.metergroup.com/Manuals/20780_PARIO_Manual_Web.pdf

Mulqueen J, Stafford J.V., Tanner D.W., 1977. “Evaluation of penetrometers for measuring soil strength. J. Terramechanics.” 14(3). 137-151. Web.

Piepho, Hans-Peter, 2019. “A Coefficient of Determination (R2) for Generalized Linear Mixed Models.” Biometrical journal 61.4 (2019): 860–872. Web.

Pinheiro, É.F.M.; Ceddia, M.B.; Clingensmith, C.M.; Grunwald, S.; Vasques, G.M. “Prediction of Soil Physical and Chemical Properties by Visible and Near-Infrared Diffuse Reflectance Spectroscopy in the Central Amazon.” Remote Sens. 2017, 9, 293. https://doi.org/10.3390/rs9040293

Prevost, M. “Predicting Soil Properties from Organic Matter Content Following Mechanical Site Preparation of Forest Soils.” Soil Science Society of America journal 68.3 (2004): 943–949. Web.

Reid, H., 2014. Introduction to statistics: Fundamental Concepts and Procedures of Data Analysis. SAGE Publications, Inc, https://dx.doi.org/10.4135/9781071878927

Riza, Sativandi, et al. “Modeling Soil Landscapes and Soil Textures Using Hyperscale Terrain Attributes.” Geoderma 402 (2021): 115177–. Web.

Rula, A.A., C.J. Nuttall Jr., 1971. “An analysis of ground mobility models (ANAMOB).” Technical Report M-71-4, U.S. Army Engineer Waterways Experiment Station, Vicksburg, MS. Web

S. Paterson, B. Minasny, A.B. McBratney, 2018. “Spatial variability of Australian soil texture: a multiscale analysis.” Geoderma, 309 (2018), pp. 60-74

Shahriari, Mohammad, et al. “Predicting Regional Spatial Distribution of Soil Texture in Floodplains Using Remote Sensing Data: A Case of Southeastern Iran.” Catena (Giessen) 182 (2019): 104149–. Web.

Shirazi, Mostafa A, Larry Boersma, and Colleen Burch Johnson. “Particle-Size Distributions: Comparing Texture Systems, Adding Rock, and Predicting Soil Properties.” Soil Science Society of America journal 65.2 (2001): 300–310. Web.

Stevens, Stevens Water Monitoring Systems, Inc. 2018. HydraProbe Soil Sensor User’s Manual Rev. VI. https://stevenswater.com/products/hydraprobe/

Tarboton , David G., (2004), “Terrain Analysis Using Digital Elevation Models (TauDEM).” Utah State University. https://hydrology.usu.edu/taudem/taudem5/index.html

Vermote, E., Justice, C., Claverie, M., & Franch, B. (2016). “Preliminary analysis of the performance of the Landsat 8/OLI land surface reflectance product.” Remote Sensing of Environment, 185, 46-56.

Wong, J.Y., 1980. “Data processing methodology in the characterization of the mechanical properties of terrain.” J. Terramechanics. 17(1). 13-41. doi:10.1016/0022-4898(80)90014-2

Wong, J.Y., 2010. “Terramechanics and Off-Road Vehicle Engineering.” 2nd Ed. Elsevier, Oxford, UK.

Z. Wang, W. Shi, 2017. “Mapping soil particle-size fractions: a comparison of compositional kriging and log-ratio kriging.” J. Hydrol., 546 (2017), pp. 526-541. Doi: 10.1016/j.jhydrol.2017.01.029